Aperture Photometry on PLATO Target Stars

5th forum of Action Fédératrice Etoiles (AFE)

l'Observatoire de Paris — LESIA

Laboratoire d'Études Spatiales et d'Instrumentation en Astrophysique

Escola Politécnica da USP

USP UNIVERSITY OF SÃO PAULO

Plato DPA-WG

Victor MARCHIORI

victor.marchiori@obspm.fr

(LESIA – POLE ETOILE)

Réza SAMADI (LESIA), Fábio FIALHO (EPUSP)

MEUDON – 13/11/2017

Overview

- The PLATO Mission
  - Main science goals
  - Instrument characteristics
  - Science requirements
- Data processing chain: instrument calibration and correction algorithms
- PLATO's on-board photometry problematic
- Contaminant star flux on the on-board photometry
- Mitigation of contaminant flux in the on-board lightcurves

The PLATO Mission: overview

- A medium size (M3) mission of the ESA's Cosmic Vision Program expected to be launched by 2026 in L2 orbit

The PLATO Mission: overview

- A medium size (M3) mission of the ESA's Cosmic Vision Program expected to be launched by 2026 in L2 orbit
- Main science goals
  - Build a statistically significant sample of planets down to Earth-size orbiting main sequence F, G, K Solar-type stars and M-stars in their habitable zone. Stars magnitude range: $4 \leq m_V \leq 16$

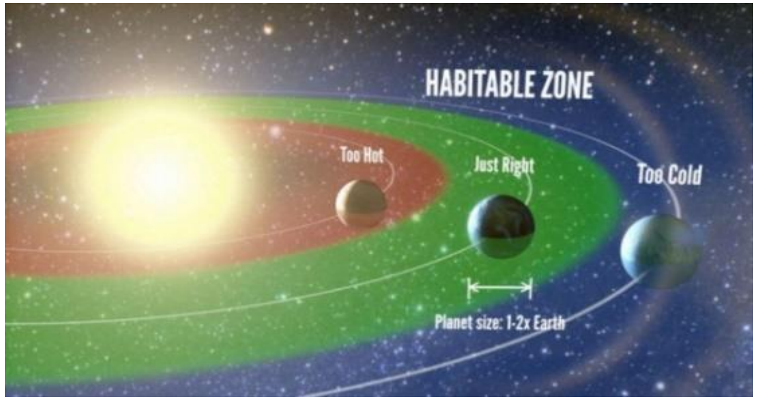

The PLATO Mission: overview

- A medium size (M3) mission of the ESA's Cosmic Vision Program expected to be launched by 2026 in L2 orbit
- Main science goals
  - Build a statistically significant sample of planets down to Earth-size orbiting main sequence F, G, K Solar-type stars and M-stars in their habitable zone. Stars magnitude range: $4 \leq m_V \leq 16$
  - Planet detection and accurate (a few percent) radius determination from photometric transits

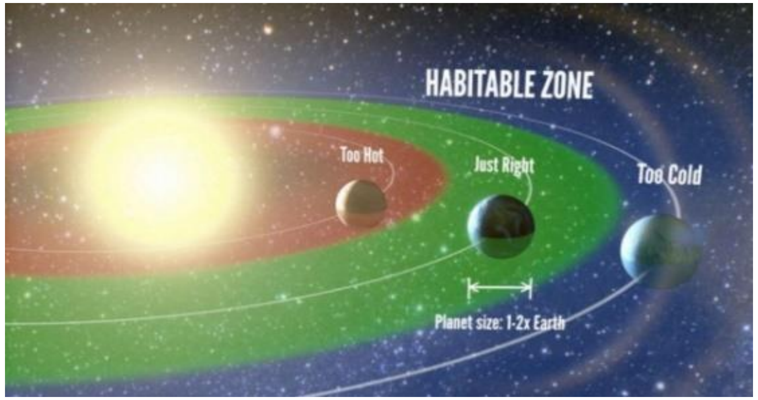

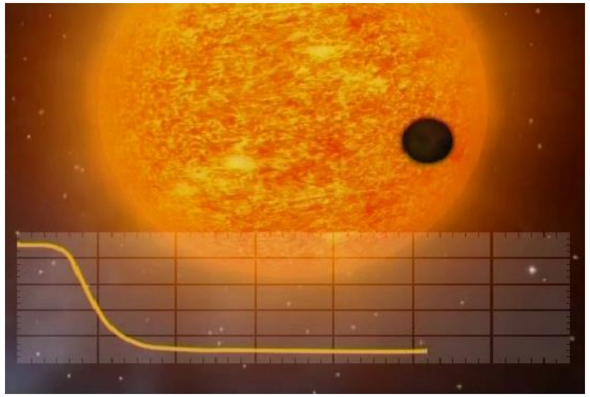

The PLATO Mission: overview

- A medium size (M3) mission of the ESA's Cosmic Vision Program expected to be launched by 2026 in L2 orbit
- Main science goals
    - Build a statistically significant sample of planets down to Earth-size orbiting main sequence F, G, K Solar-type stars and M-stars in their habitable zone. Stars magnitude range: $4 \leq m_V \leq 16$
    - Planet detection and accurate (a few percent) radius determination from photometric transits
    - Accurate (a few percent) planet masses determination from ground-based radial velocity follow-up

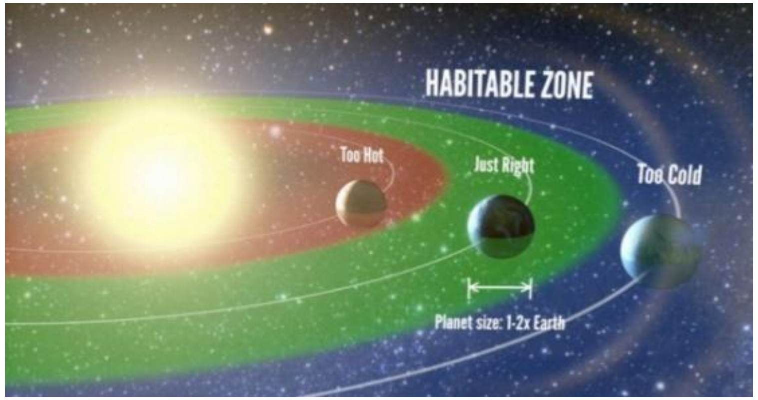

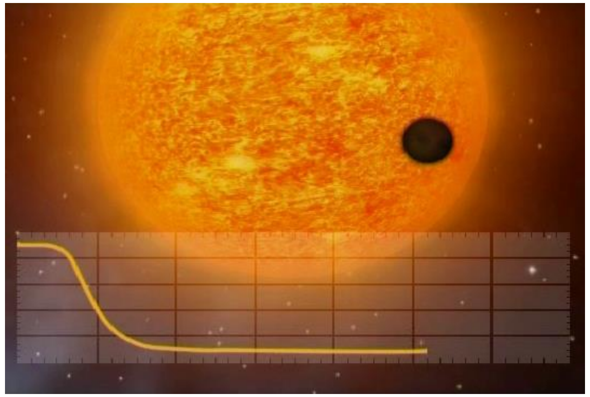

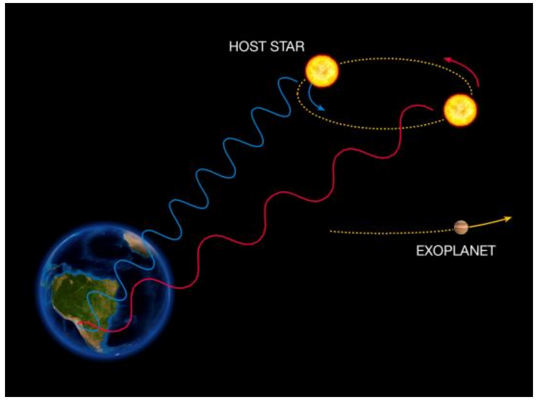

The PLATO Mission: overview

- A medium size (M3) mission of the ESA's Cosmic Vision Program expected to be launched by 2026 in L2 orbit
- Main science goals
  - Build a statistically significant sample of planets down to Earth-size orbiting main sequence F, G, K Solar-type stars and M-stars in their habitable zone. Stars magnitude range: $4 \leq m_V \leq 16$
  - Planet detection and accurate (a few percent) radius determination from photometric transits
  - Accurate (a few percent) planet masses determination from ground-based radial velocity follow-up
  - Stellar masses and radii determination to an accuracy of a few percent from asteroseismology
  - Stellar age determination to an accuracy better than 10% from asteroseismology

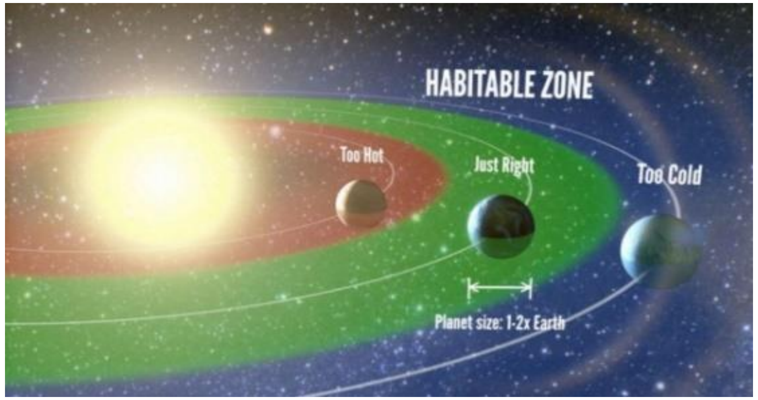

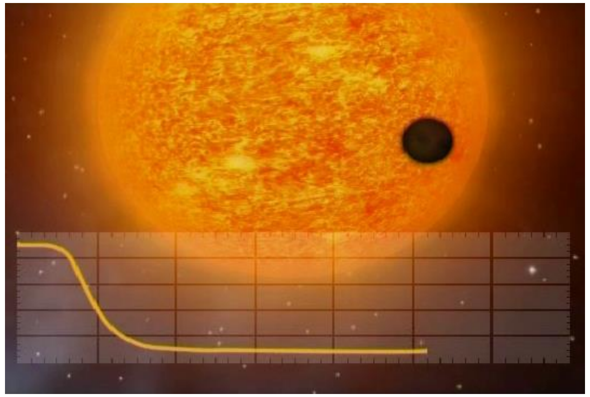

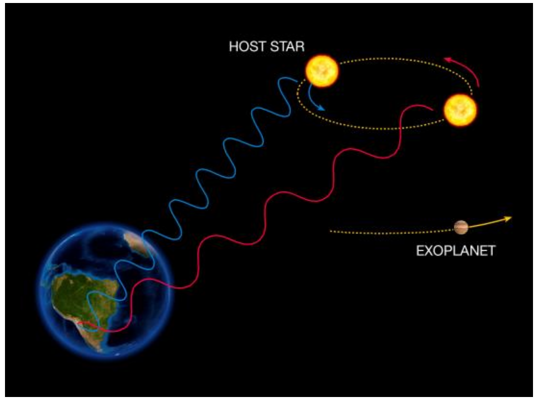

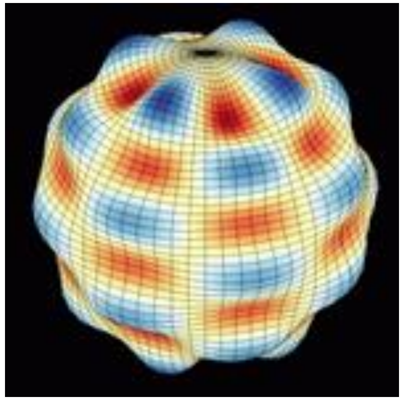

The PLATO Mission: instrument

- Instrument: multi-telescope concept
  - 2 "fast" (2.5 seconds cadence) telescopes for Attitude and Orbit Control System
  - 24 "normal" (25 seconds cadence) telescopes for the core science
  - Field of View (FoV): $\cong 2300\ \text{deg}^2$

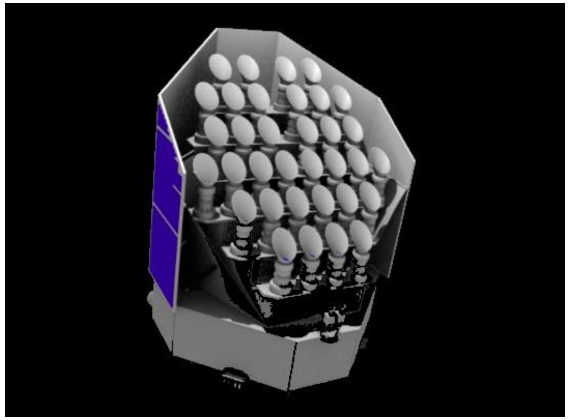

The PLATO Mission: instrument

- Instrument: multi-telescope concept
  - 2 “fast” (2.5 seconds cadence) telescopes for Attitude and Orbit Control System
  - 24 “normal” (25 seconds cadence) telescopes for the core science
  - Field of View (FoV): ≅ 2300 deg^2
  - Characteristics of each telescope (camera):
    - ≅ 1100 deg^2 FoV with 120mm pupil and fully dioptric design (6 lenses)

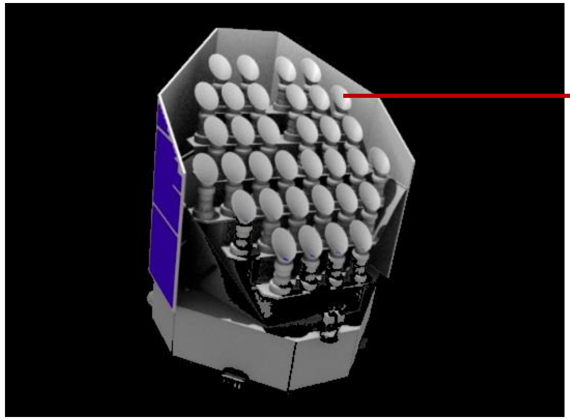

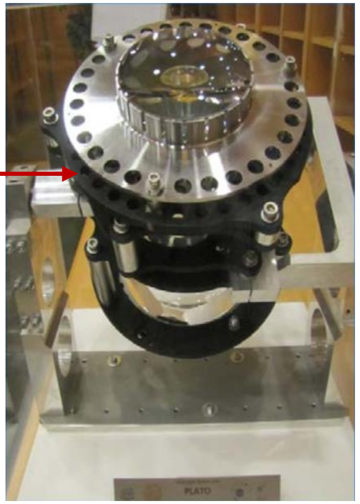

The PLATO Mission: instrument

- Instrument: multi-telescope concept
  - 2 “fast” (2.5 seconds cadence) telescopes for Attitude and Orbit Control System
  - 24 “normal” (25 seconds cadence) telescopes for the core science
  - Field of View (FoV): ≅ 2300 deg^2
  - Characteristics of each telescope (camera):
    - ≅ 1100 deg^2 FoV with 120mm pupil and fully dioptric design (6 lenses)
    - Four CCDs (detectors) with 4510×4510 $18\mu m$ pixels each
    - Wavelength band: 500−1000 nm

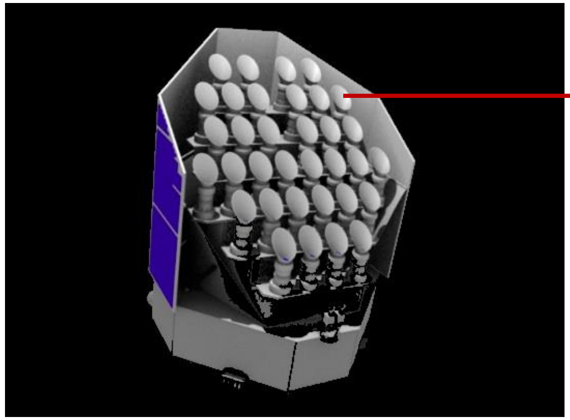

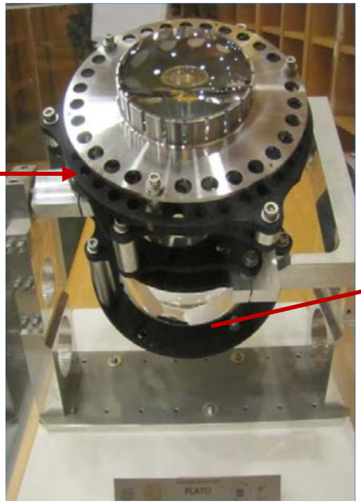

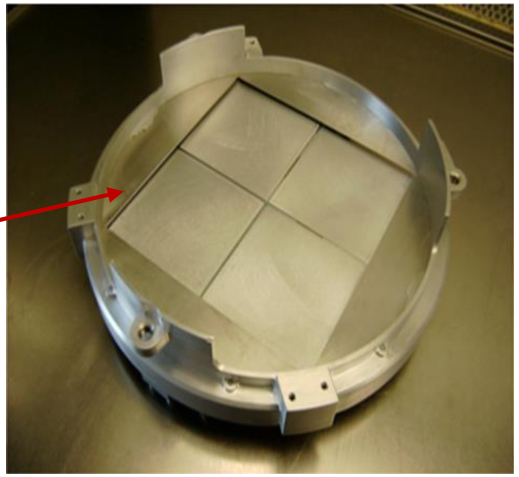

The PLATO Mission: science requirements

- PLATO science goals achievement will depend on high photometric stability (up to 2 years observations) and ultra-high photometric precision

The PLATO Mission: science requirements

- PLATO science goals achievement will depend on high photometric stability (up to 2 years observations) and ultra-high photometric precision

- Asteroseismology noise requirements
  - 34 ppm in 1 hour to detect short life-time solar-like oscillations of dwarf stars at $m_v \leq 11$

The PLATO Mission: science requirements

- PLATO science goals achievement will depend on high photometric stability (up to 2 years observations) and ultra-high photometric precision

- Asteroseismology noise requirements
  - 34 ppm in 1 hour to detect short life-time solar-like oscillations of dwarf stars at $m_V \leq 11$

- Planetary transit noise requirements
  - 80 ppm in 1 hour to detect Earth-like planets orbiting the habitable zone of $m_V \leq 13$ stars

The PLATO Mission: science requirements

- Total residual noise must be dominated by the photon noise from target stars

The PLATO Mission: science requirements

- Total residual noise must be dominated by the photon noise from target stars
- Systematic error residuals must be limited to 1/3 of random noise

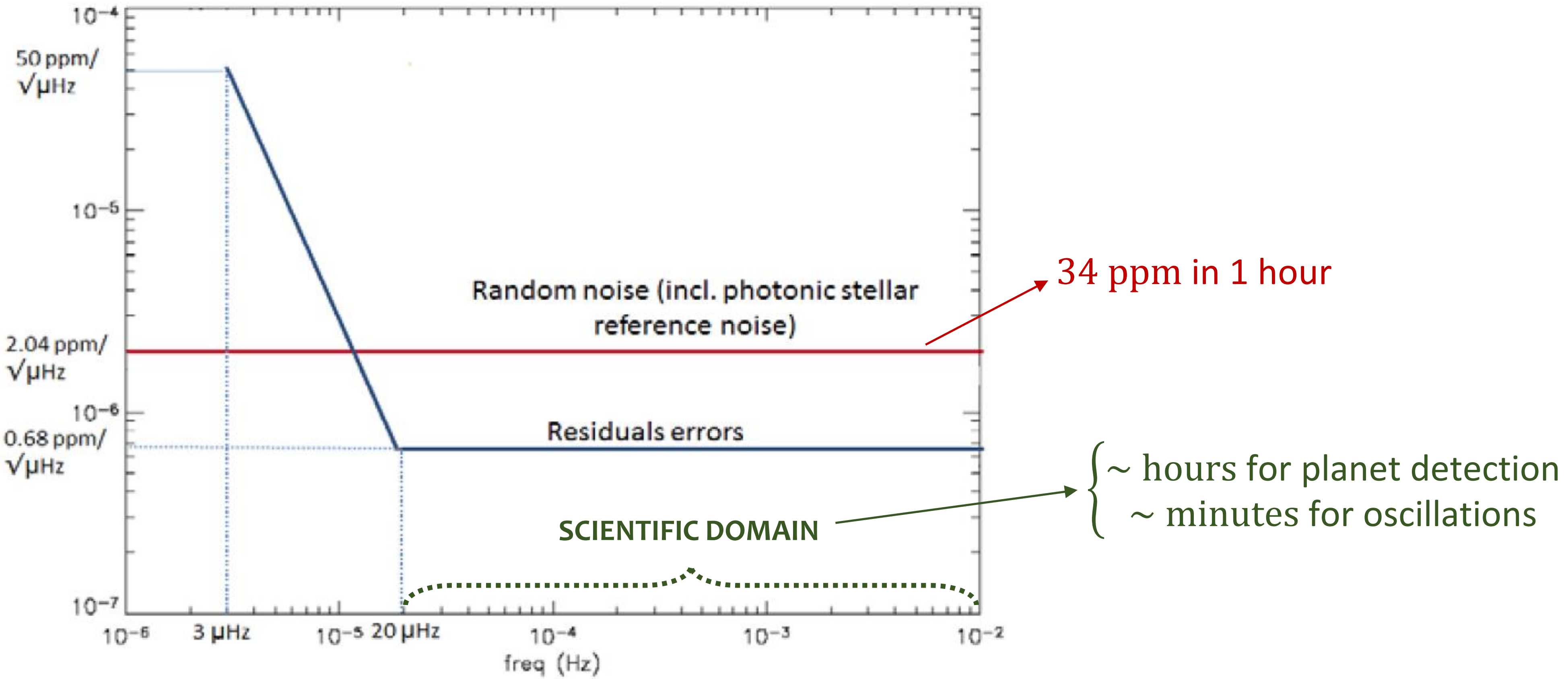

Data processing chain: instrument calibration and correction algorithms

- Main sources of noise and systematic errors
  - Detectors: Charge Transfer Inefficiency (CTI), brighter-fatter effect
  - Pointing: jitter
  - Platform: thermoelastic distortion (multi-telescopes approach)
  - Natural: kinematic aberration, sky background, contaminant stars

Data processing chain: instrument calibration and correction algorithms

- Main sources of noise and systematic errors
  - Detectors: Charge Transfer Inefficiency (CTI), brighter-fatter effect
  - Pointing: jitter
  - Platform: thermoelastic distortion (multi-telescopes approach)
  - Natural: kinematic aberration, sky background, contaminant stars

- In order to derive lightcurves within noise requirements, several on-board and on-ground calibration/correction algorithms are needed

Data processing chain: instrument calibration and correction algorithms

- Main sources of noise and systematic errors
  - Detectors: Charge Transfer Inefficiency (CTI), brighter-fatter effect
  - Pointing: jitter
  - Platform: thermoelastic distortion (multi-telescopes approach)
  - Natural: kinematic aberration, sky background, contaminant stars

- In order to derive lightcurves within noise requirements, several on-board and on-ground calibration/correction algorithms are needed

- Constraints: limitation of telemetry and on-board CPU budgets

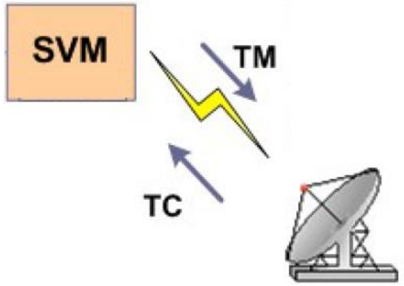

Data processing chain: instrument calibration and correction algorithms

- Main sources of noise and systematic errors
  - Detectors: Charge Transfer Inefficiency (CTI), brighter-fatter effect
  - Pointing: jitter
  - Platform: thermoelastic distortion (multi-telescopes approach)
  - Natural: kinematic aberration, sky background, contaminant stars

- In order to derive lightcurves within noise requirements, several on-board and on-ground calibration/correction algorithms are needed

- Constraints: limitation of telemetry and on-board CPU budgets

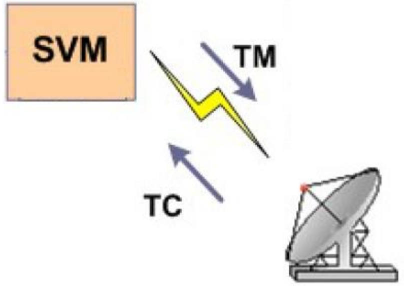

- On-board photometry required for the majority of the target stars

Data processing chain: instrument calibration and correction algorithms

- Main sources of noise and systematic errors
  - Detectors: Charge Transfer Inefficiency (CTI), brighter-fatter effect
  - Pointing: jitter
  - Platform: thermoelastic distortion (multi-telescopes approach)
  - Natural: kinematic aberration, sky background, contaminant stars

- In order to derive lightcurves within noise requirements, several on-board and on-ground calibration/correction algorithms are needed

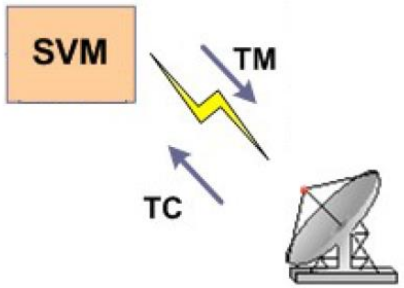

- Constraints: limitation of telemetry and on-board CPU budgets

- On-board photometry required for the majority of the target stars
  - Aperture (mask-based) photometry presents the best compromise between Noise-To-Signal Ratio (NSR) and computational cost

Satellite on-board photometry: aperture masks

- Principle

IMAGE
(STAR + BACKGROUND)

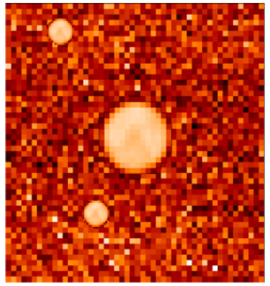

MASK

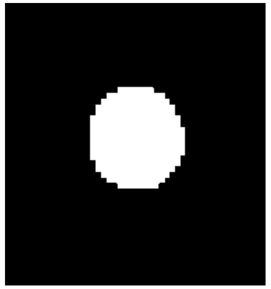

$$F(i) = \sum [\ \text{IMAGE} \times \text{MASK}\ ]$$

$$F(t) =$$

LIGHTCURVE

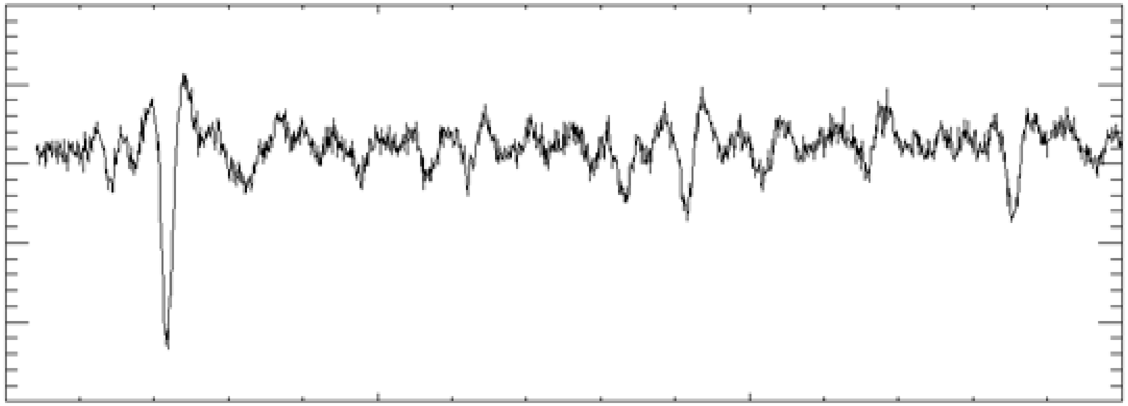

Satellite on-board photometry: aperture masks

- Principle

$$F(i) = \sum [\ \text{IMAGE (STAR + BACKGROUND)} \times \text{MASK}\ ]$$

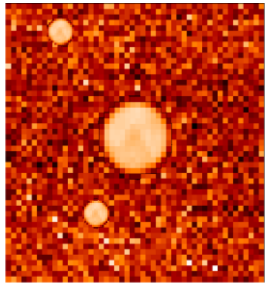

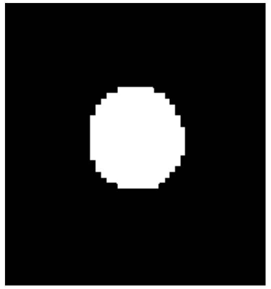

$F(t) =$

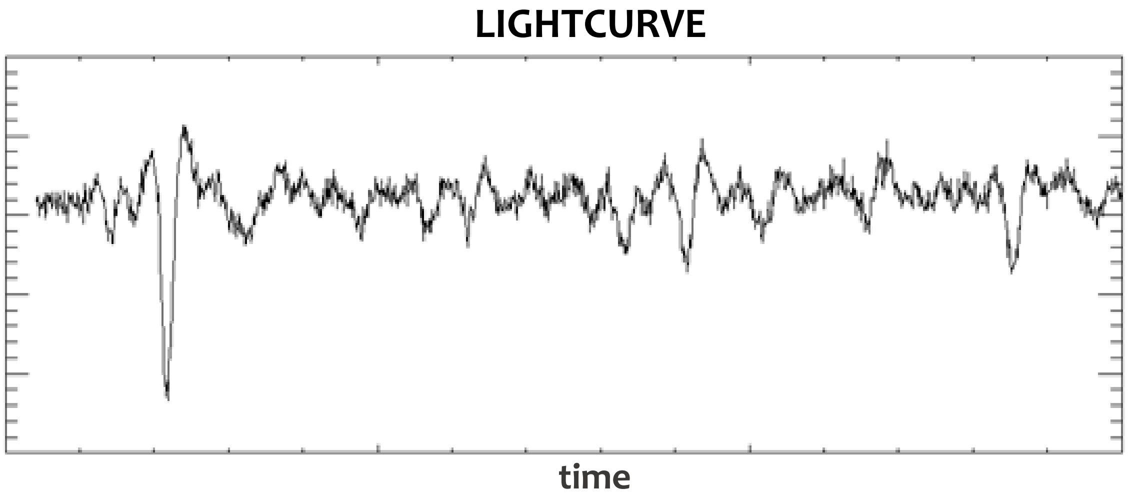

- Objective: develop optimized aperture photometry masks models
  - Provide the lowest possible NSR
  - Minimize the presence of contaminant flux
  - Constrain payload CPU, memory and telemetry
  - Limit as well as possible the residuals to be corrected on-ground

Measuring aperture masks performance

- Signal-to-Noise Ratio (SNR)

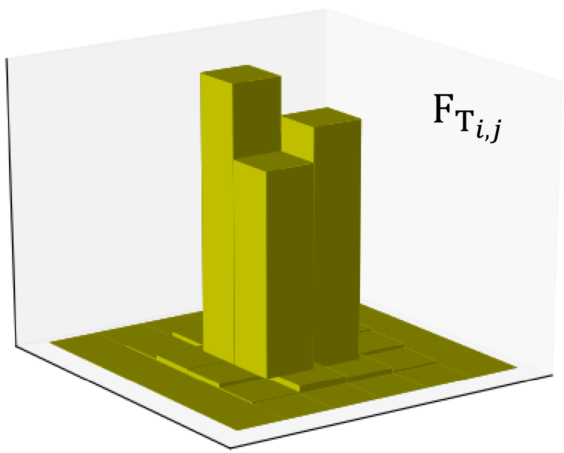

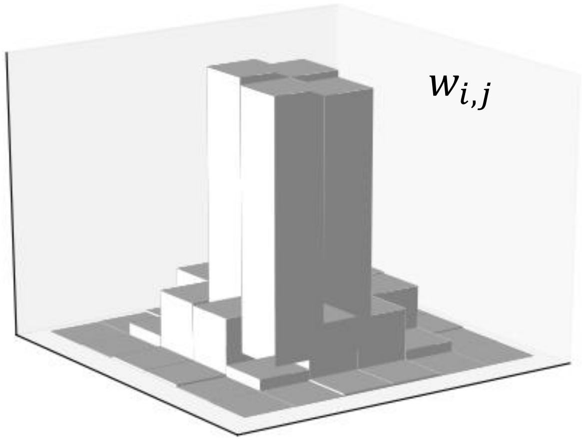

$$\mathrm{SNR} = \frac{\sum_{i,j}\left(F_{T_{i,j}} \times w_{i,j}\right)}{\sqrt{\sum_{i,j}\left(F_{T_{i,j}} \times w_{i,j}^2\right) + \sum_{i,j}\left(B_{i,j} \times w_{i,j}^2\right) + \sum_{i,j}\left(R_{i,j}^2 \times w_{i,j}^2\right)}}$$

$F_{T_{i,j}}$ = target star flux at pixel (i, j)

$w_{i,j}$ = mask weigth at pixel (i, j)

$B_{i,j}$ = background noise at pixel (i, j)

$R_{i,j}$ = readout noise at pixel (i, j)

Measuring aperture masks performance

- Contamination rate (τ_C)

TARGET + CONTAMINANT STARS SIGNAL

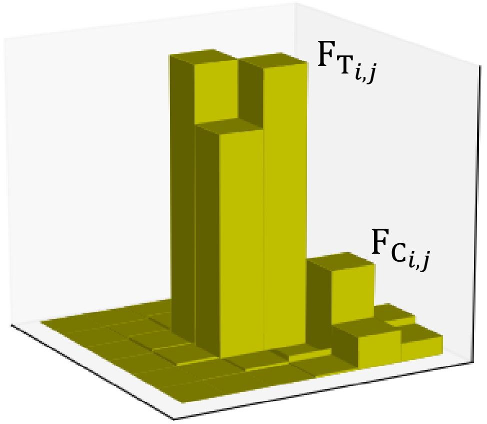

MASK

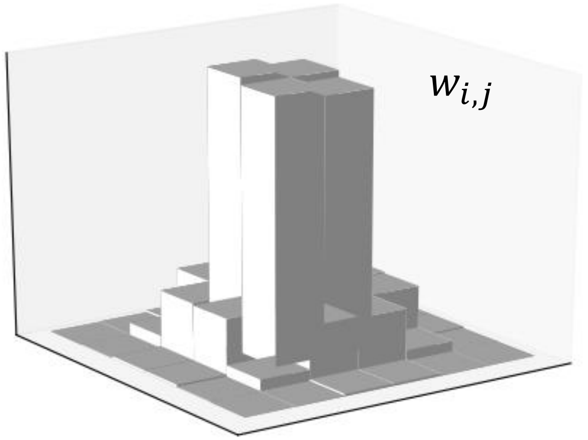

$$\tau_C = \frac{\sum_{i,j}\left(F_{C_{i,j}} \times w_{i,j}\right)}{\sum_{i,j}\left[\left(F_{T_{i,j}} + F_{C_{i,j}}\right) \times w_{i,j}\right]}$$

$$(0 \leq \tau_C \leq 1)$$

$F_{C_{i,j}}$ = contaminant star flux at pixel (i, j)

$F_{T_{i,j}}$ = target star flux at pixel (i, j)

$w_{i,j}$ = mask weight at pixel (i, j)

PSF Enclosure energy

- At detector level, star flux are translated into low spatial resolution images called imagettes

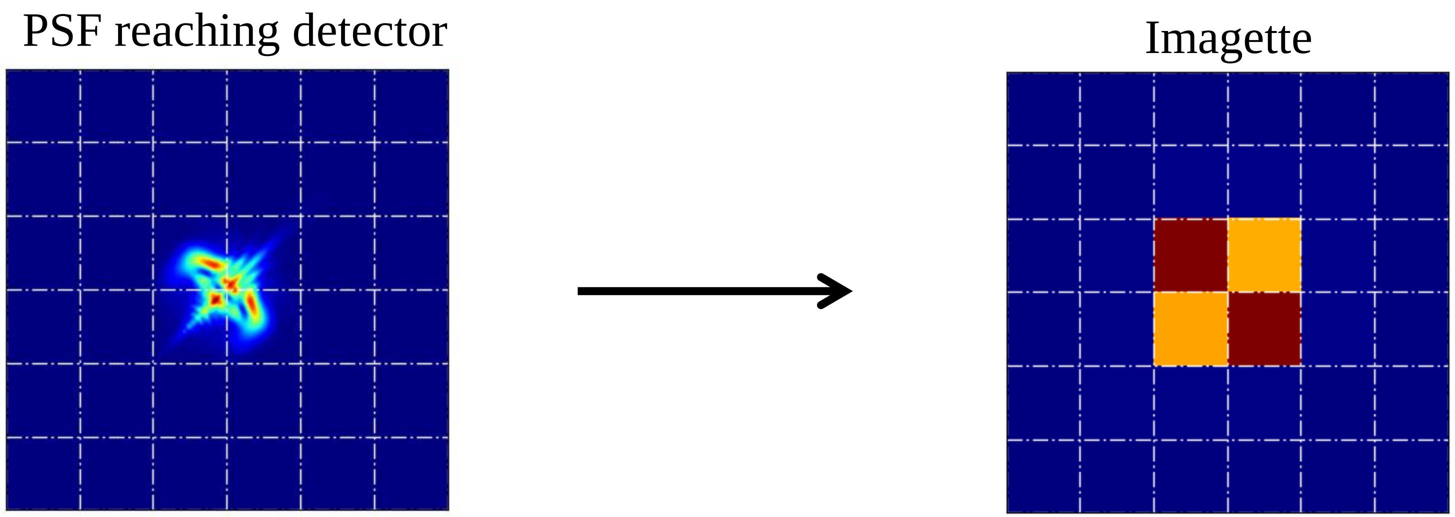

PSF Enclosure energy

- At detector level, star flux are translated into low spatial resolution images called imagettes

PSF reaching detector

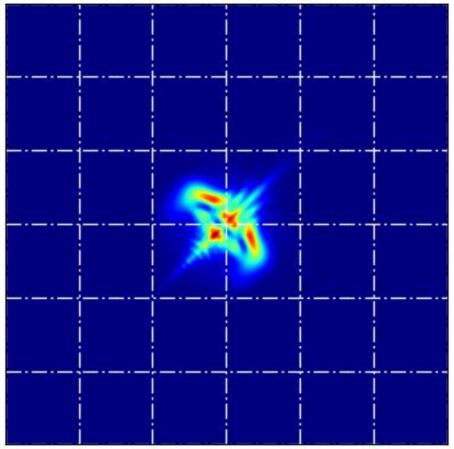

Imagette

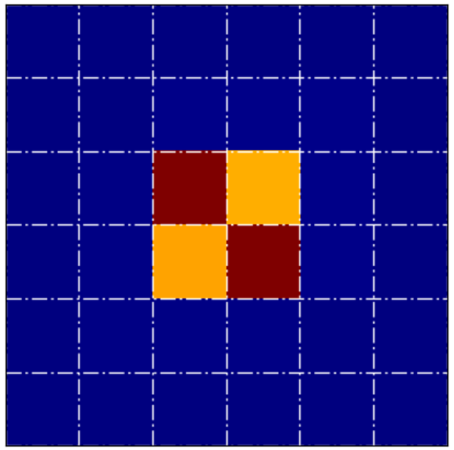

- 90% of the PSF energy is concentrated within about 4 pixels of the CCDs
  - Increases the number of observed stars
  - Reduces overlap of target and contaminant flux
  - Increases SNR (in a large sense)
  - Aperture photometry performance: higher sensibility to star position drift

Long-term drift of star centroids

- Thermoelastic distortion and kinematic aberration may primarily account for star centroid displacements that can reach up to 1.3 pixel over 3 months (worst case)

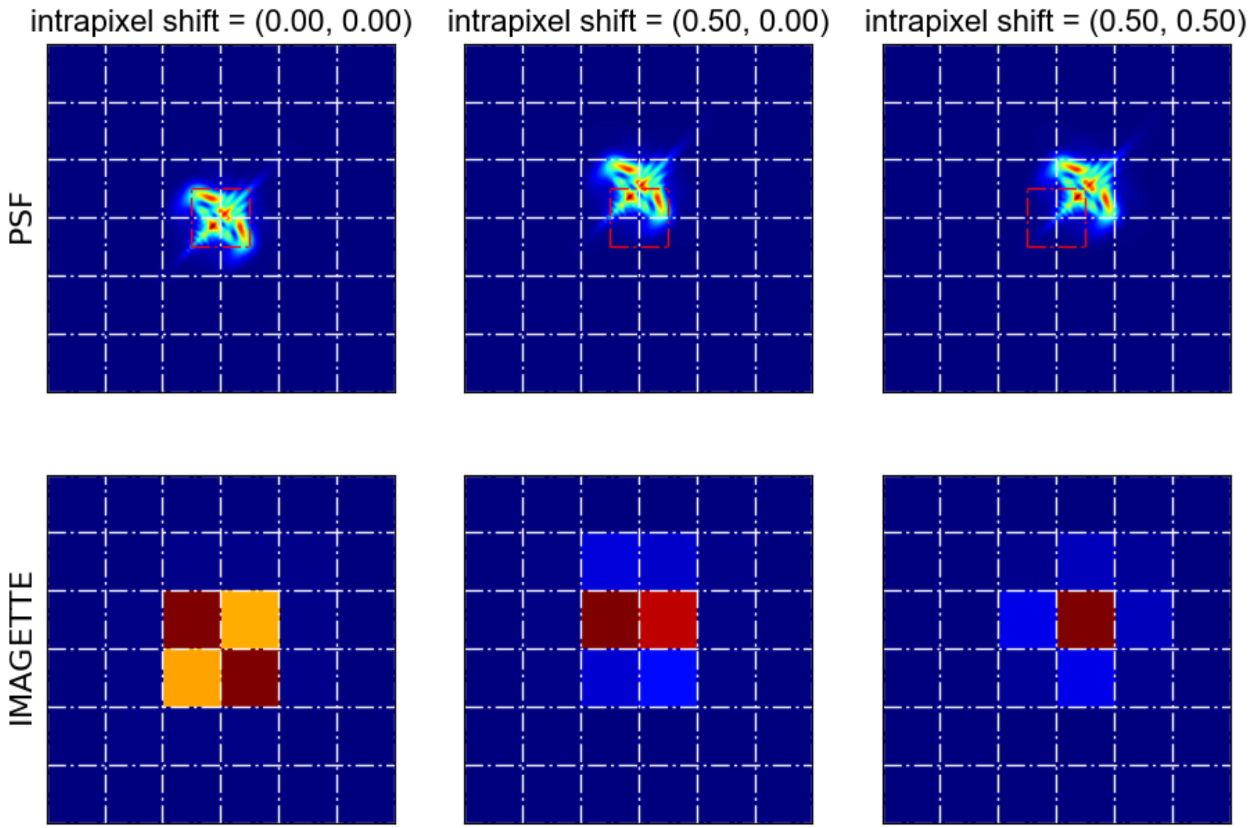

Long-term drift of star centroids

- Thermoelastic distortion and kinematic aberration may primarily account for star centroid displacements that can reach up to 1.3 pixel over 3 months (worst case)

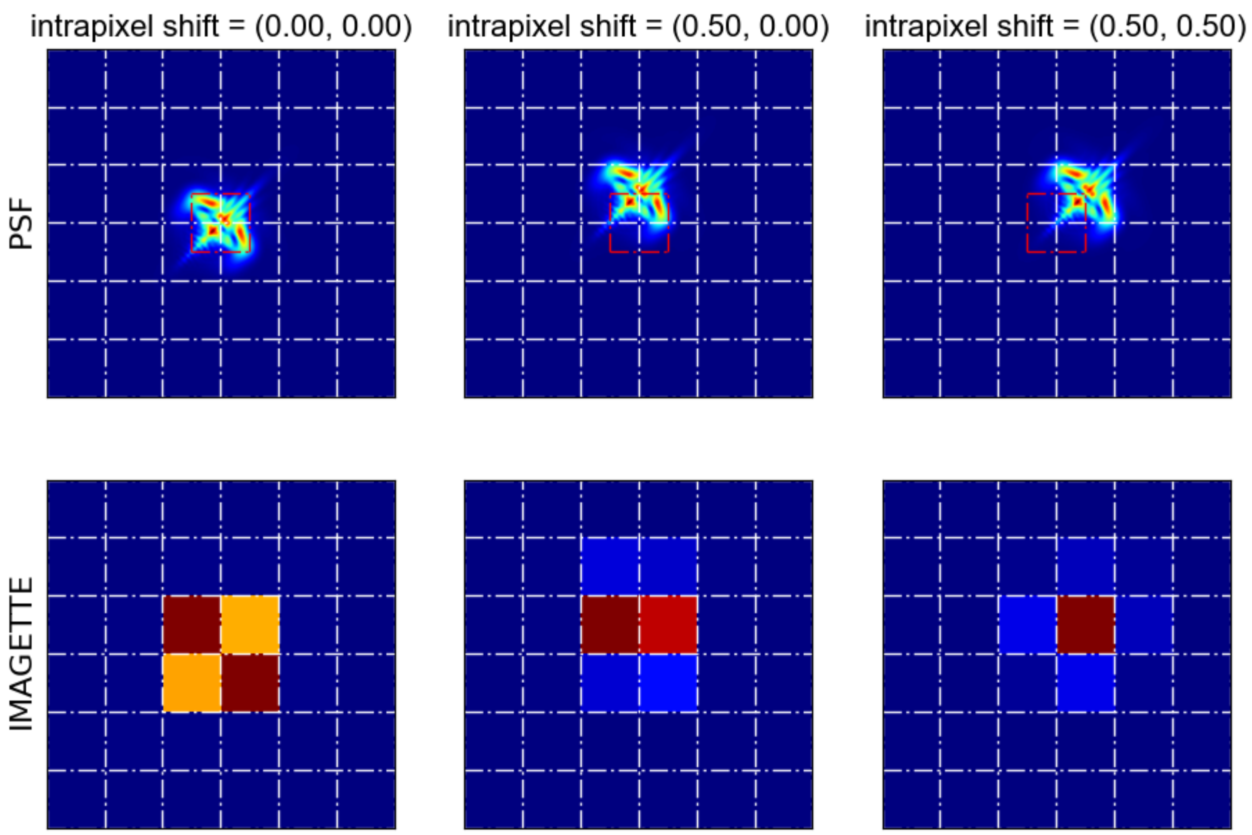

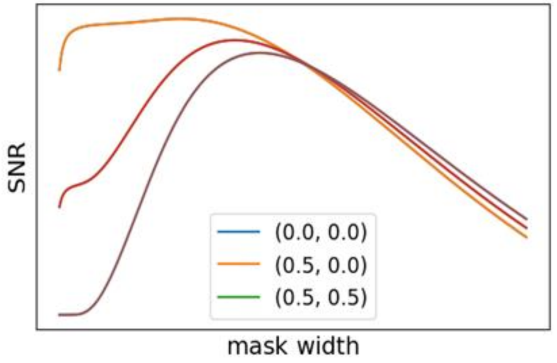

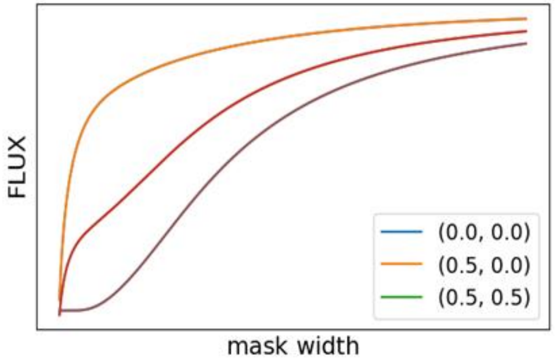

Long-term drift of star centroids

- Thermoelastic distortion and kinematic aberration may primarily account for star centroid displacements that can reach up to 1.3 pixel over 3 months (worst case)

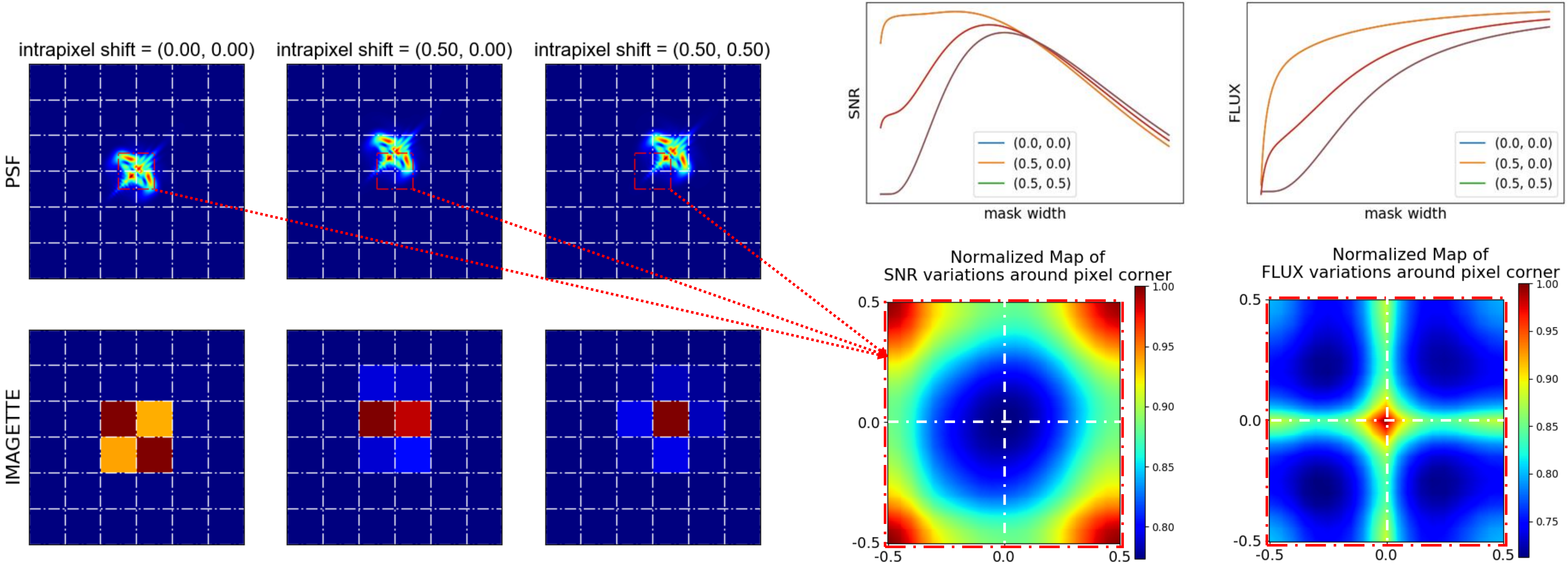

Analysis of masks performances: methodology

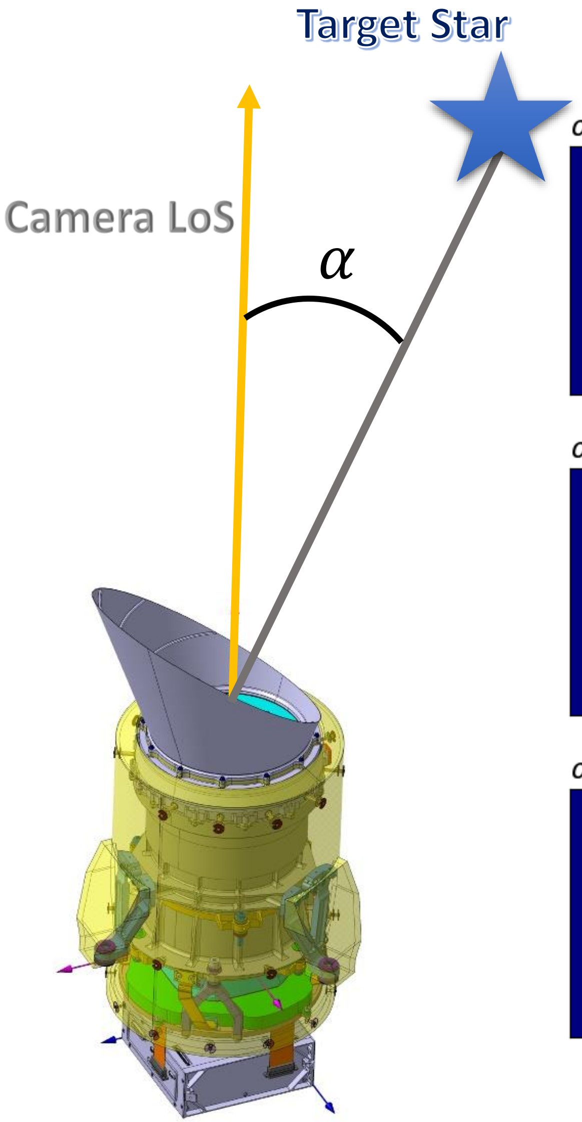

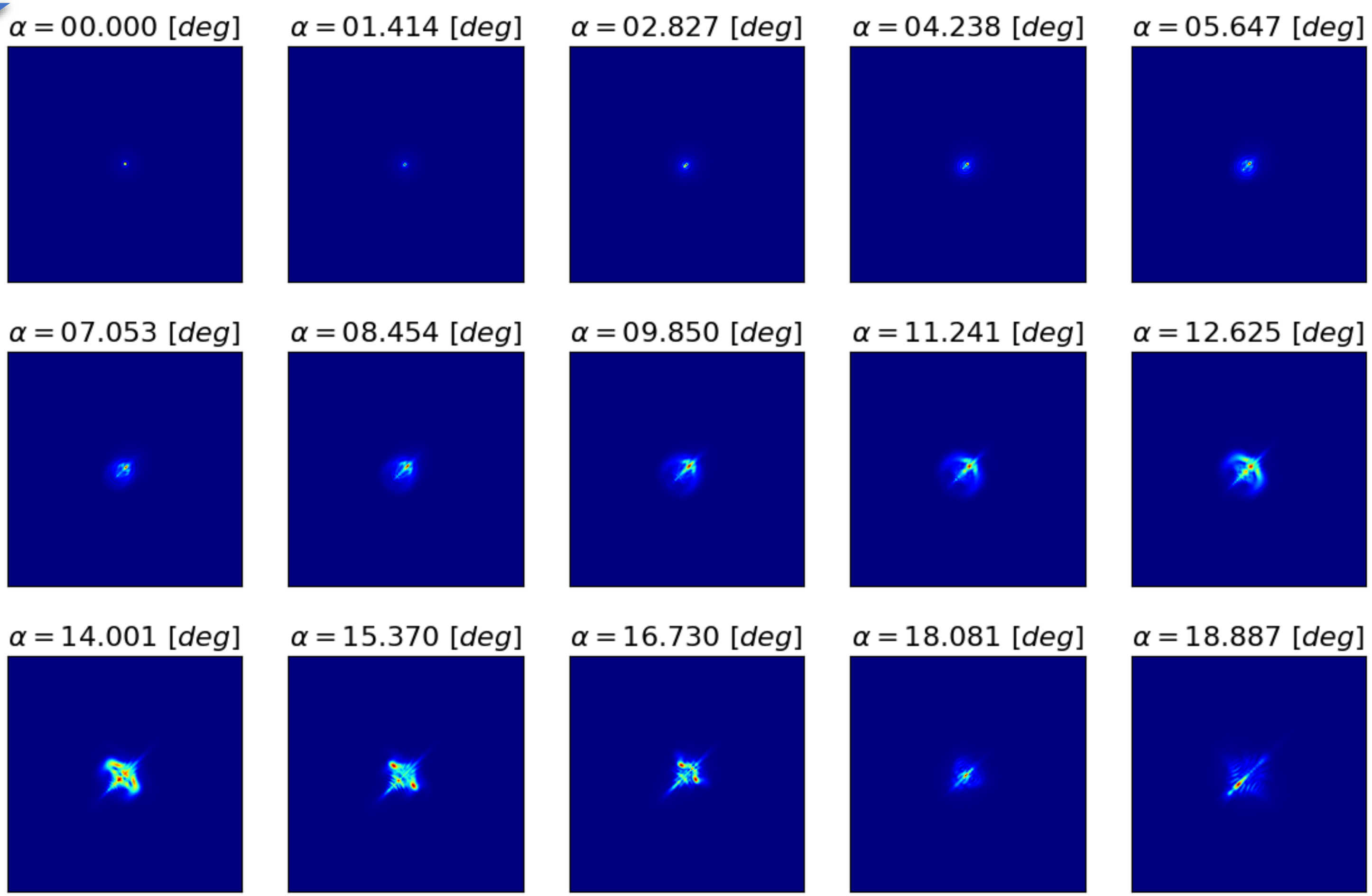

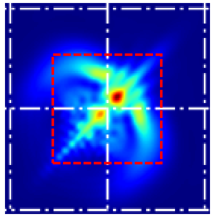

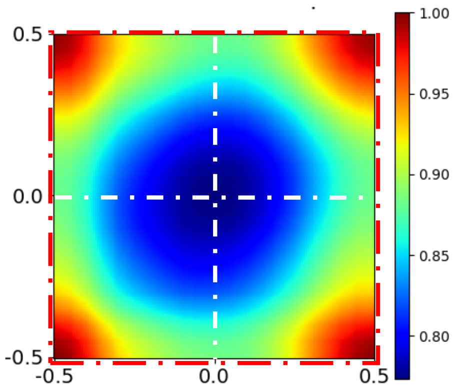

$21 \times 21 = 441$
intrapixel positions per target star position

TOTAL: $15 \times 441 = 6615$ intrapixel positions

Analysis of masks performances: methodology

TARGET STAR ONLY

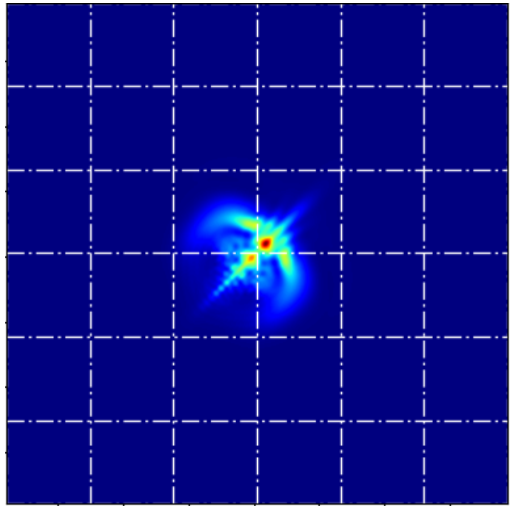

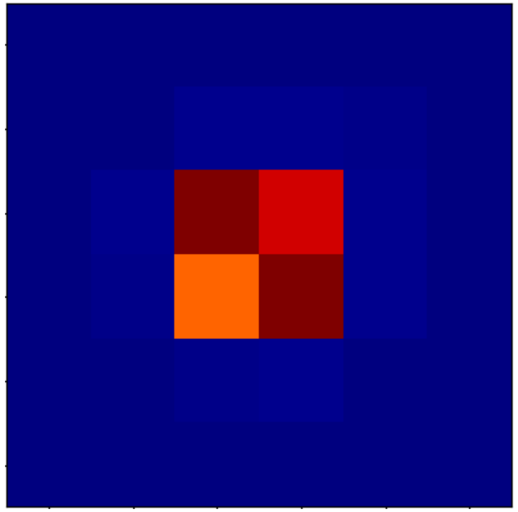

UTILIZED TO COMPUTE

MASK

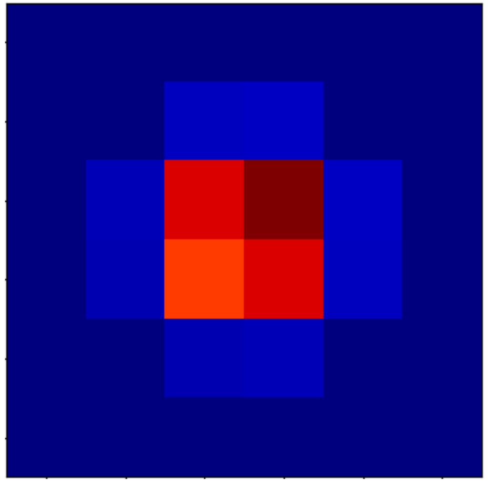

APPLIED TO

TARGET + CONTAMINANT STARS

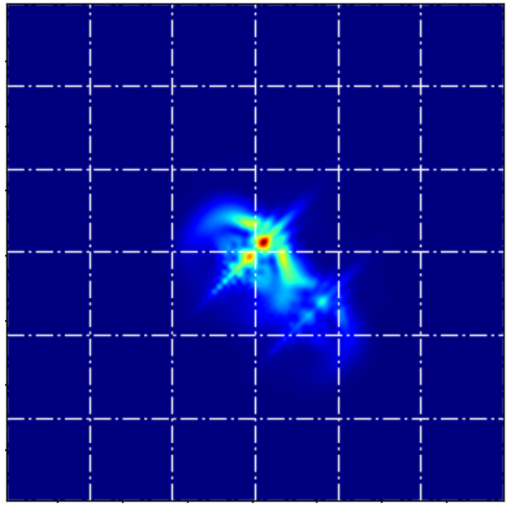

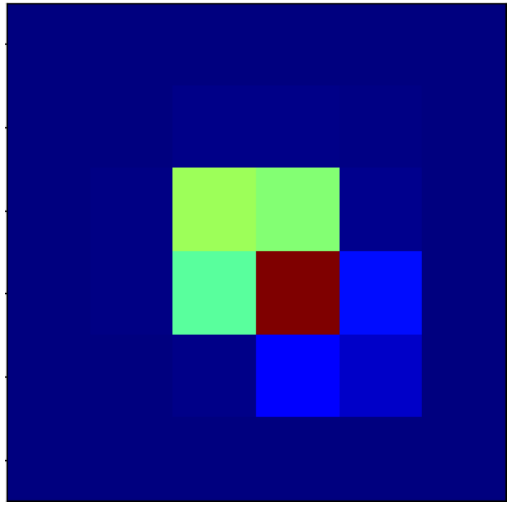

Target star parameters:
$m_v = 10.7$ and $T = 6000[K]$
Contaminant star parameters:
$m_v = 11.7$ and $T = 6000[K]$
Evaluated distances:
[0.5, 1.0, 1,5, 2.0, 2,5, 3.0] pixel(s)

Analysis of masks performances: results

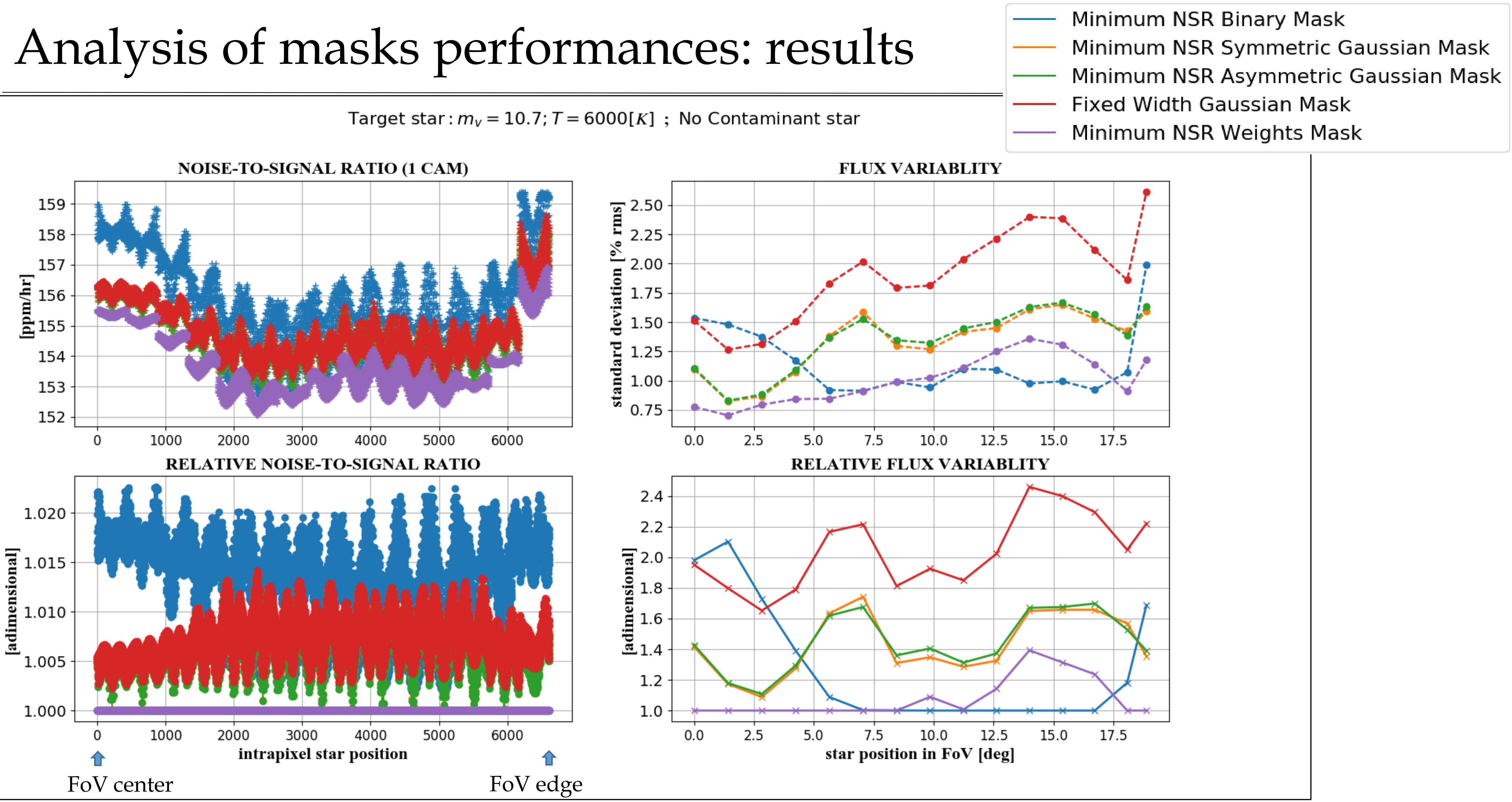

Analysis of masks performances: results

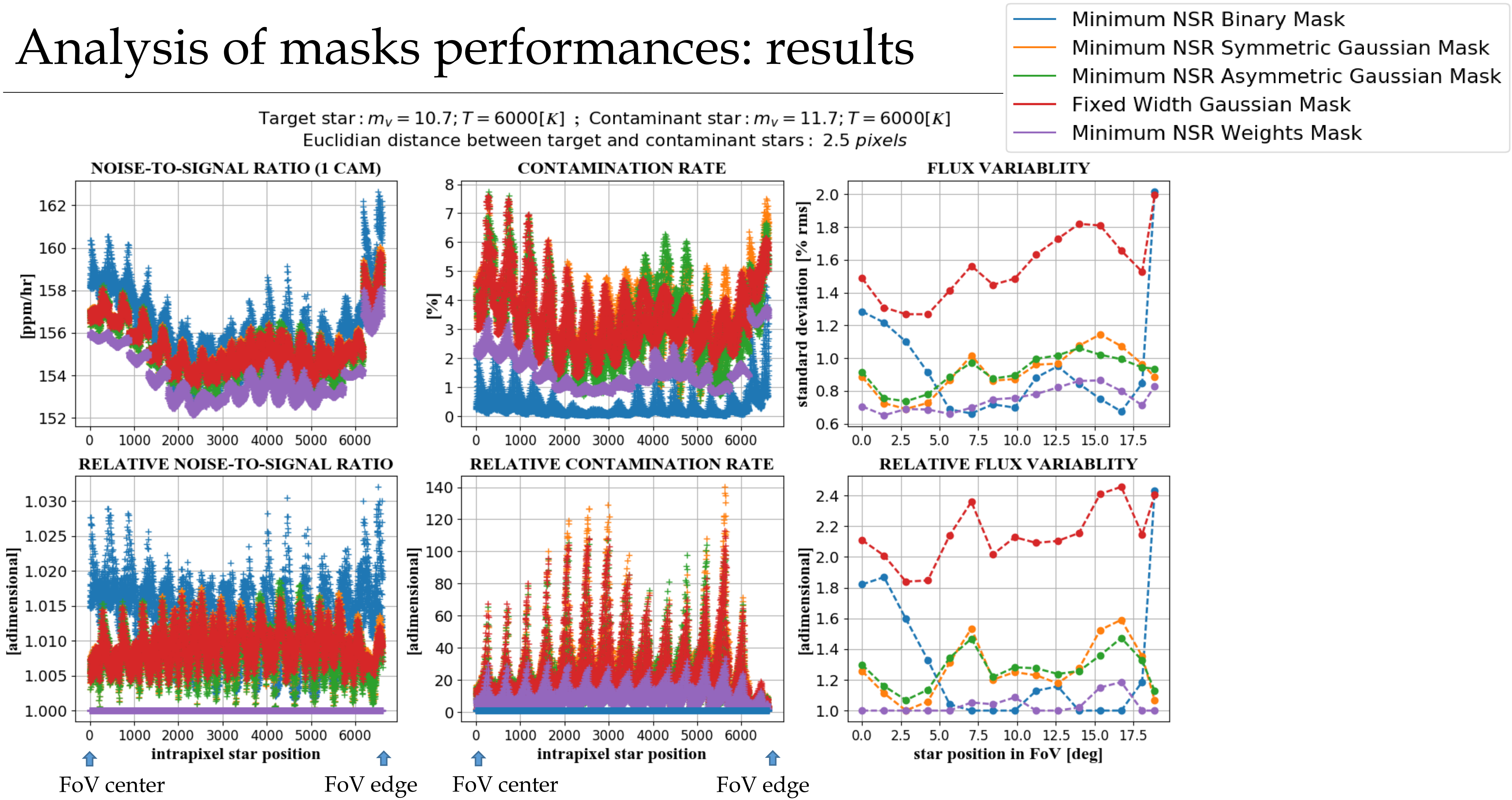

Analysis of masks performances

- **Overall** results
  - Target star: $m_V = 10.7, \ T = 6000[K]$; Contaminant star: $m_V = 11.7, T = 6000[K]$

PERFORMANCE PARAMETER	DISTANCE (target to contaminant) [pixels]	MASK MODEL				
		Optimal NSR Binary	Optimal NSR Weights	Optimal NSR Symmetric Gaussian	Optimal NSR Asymmetric Gaussian	Fixed Width Symmetric Gaussian
Relative NSR	∞	1.00 - 1.02	1.00	1.00 - 1.01	1.00 - 1.01	1.00 - 1.01
	3.0	1.00 - 1.02	1.00	1.00 - 1.01	1.00 - 1.01	1.00 - 1.01
	2.5	1.00 - 1.03	1.00	1.00 - 1.02	1.00 - 1.02	1.00 - 1.02
	2.0	1.00 - 1.08	1.00 - 1.01	1.00 - 1.03	1.00 - 1.03	1.00 - 1.03
	1.5	1.00 - 1.12	1.00 - 1.03	1.00 - 1.04	1.00 - 1.04	1.00 - 1.04
	1.0	1.00 - 1.12	1.00 - 1.04	1.00 - 1.05	1.00 - 1.05	1.00 - 1.05
	0.5	1.00 - 1.08	1.00 - 1.03	1.00 - 1.04	1.00 - 1.04	1.00 - 1.04
Relative Flux variability (STD column)	∞	1.00 - 2.10	1.00 - 1.39	1.09 - 1.74	1.11 - 1.70	1.65 - 2.46
	3.0	1.00 - 2.16	1.00 - 1.41	1.06 - 1.67	1.10 - 1.60	1.67 - 2.54
	2.5	1.00 - 2.43	1.00 - 1.19	1.00 - 1.59	1.07 - 1.47	1.84 - 2.46
	2.0	1.69 - 5.45	1.00 - 1.12	1.11 - 4.16	1.00 - 4.13	1.82 - 4.67
	1.5	3.31 - 9.29	1.00 - 1.82	1.00 - 1.58	1.00 - 1.69	1.14 - 3.66
	1.0	2.06 - 4.08	1.00 - 2.05	1.00 - 1.14	1.00 - 1.22	1.39 - 2.15
	0.5	1.20 - 2.13	1.00 - 1.29	1.00 - 2.02	1.03 - 2.01	1.44 - 2.37
Relative Contamination rate	∞	-	-	-	-	-
	3.0	1.00 - 1.06	1.00 - 25.63	2.14 - 90.46	1.57 - 81.36	1.62 - 77.03
	2.5	1.00 - 1.30	1.00 - 33.59	1.34 - 140.2	1.32 - 107.79	1.03 - 113.02
	2.0	1.00 - 1.86	1.00 - 34.14	1.02 - 115.03	1.00 - 99.85	1.00 - 101.33
	1.5	1.00 - 2.00	1.00 - 15.58	1.00 - 30.82	1.00 - 28.62	1.00 - 28.71
	1.0	1.00 - 1.73	1.00 - 3.10	1.00 - 3.54	1.00 - 3.49	1.00 - 3.67
	0.5	1.00 - 1.32	1.00 - 1.24	1.00 - 1.39	1.00 - 1.37	1.00 - 1.38

Conclusions from the presented analysis

- Noise-to-Signal Ratio: typically quite low differences among mask models
- Contamination rate: compared to binary masks, larger masks present poor performance when contaminant star is ~ 1.5 – 3.0 pixel distant from target star
- Price to pay for having narrow masks: a few percent higher NSR typically
- Price to pay for having larger masks: up to orders of magnitude higher contaminant flux depending on star position in FoV
  - Is it a concern? Yes…

Conclusions from the presented analysis

False-Transit

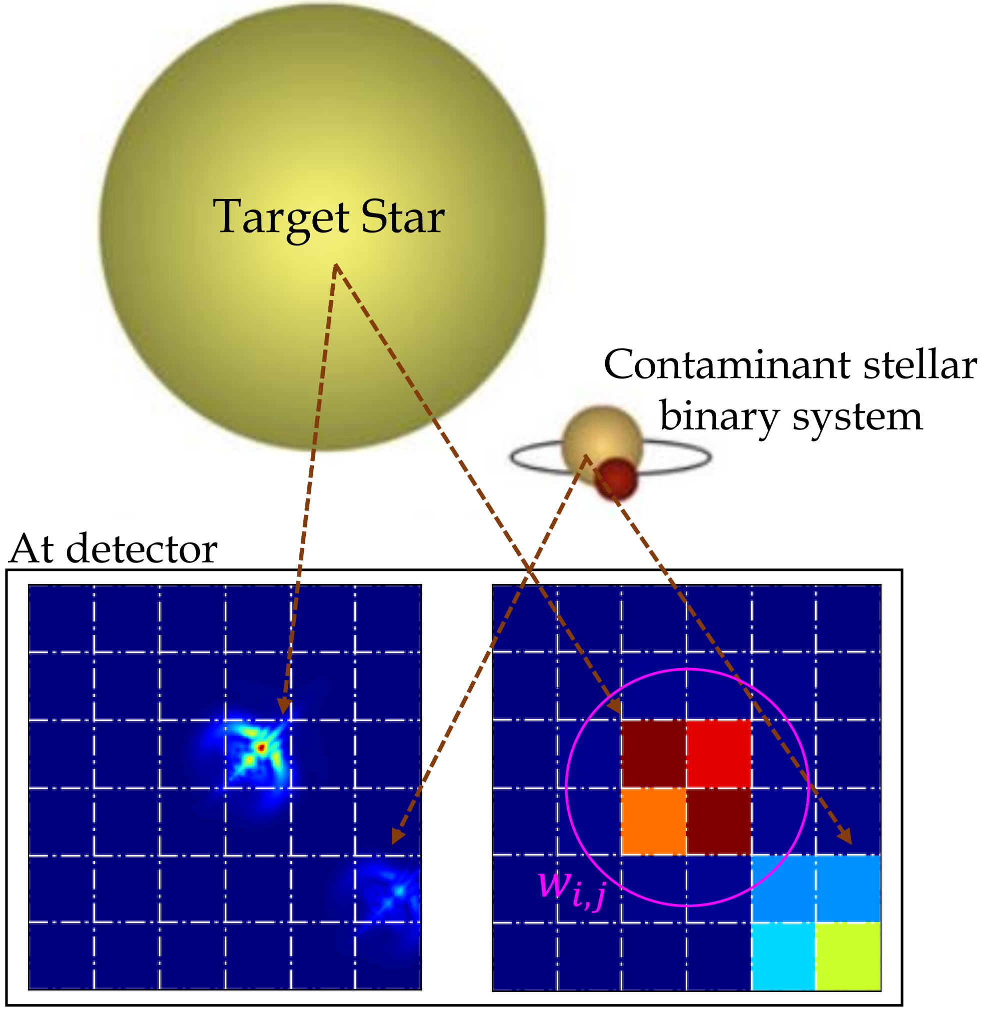

Conclusions from the presented analysis

False-Transit

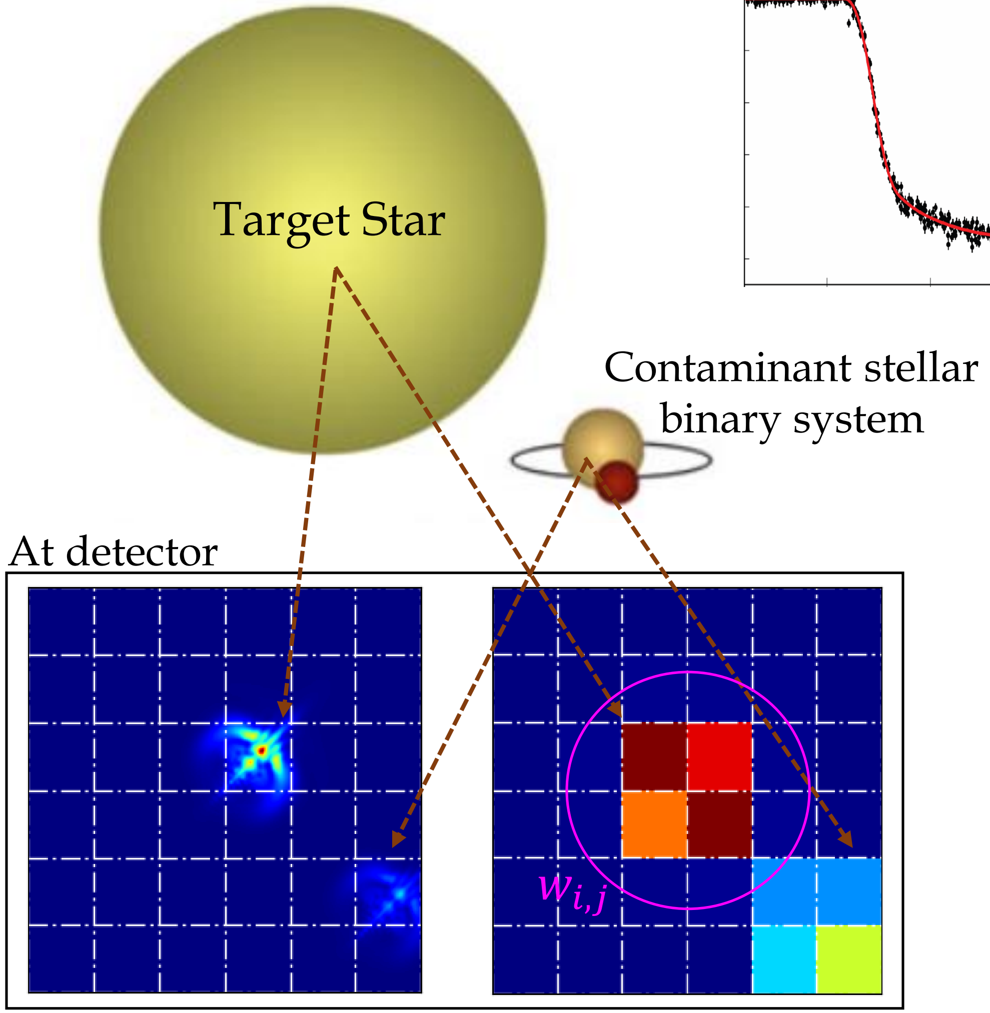

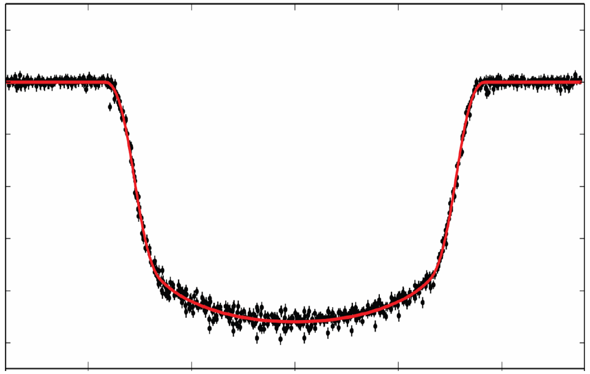

$$\delta_{obs} = \frac{\tau_C}{1-\tau_C}\left(1 - 10^{-0.4\delta_{back}}\right)$$

(δ_{back} is given in [mag] units)

Conclusions from the presented analysis

False-Transit

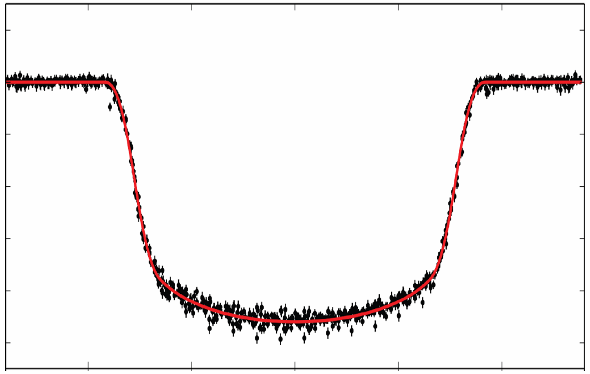

$$\delta_{obs} = \frac{\tau_C}{1-\tau_C}\left(1 - 10^{-0.4\delta_{back}}\right)$$

(δ_{back} is given in [mag] units)

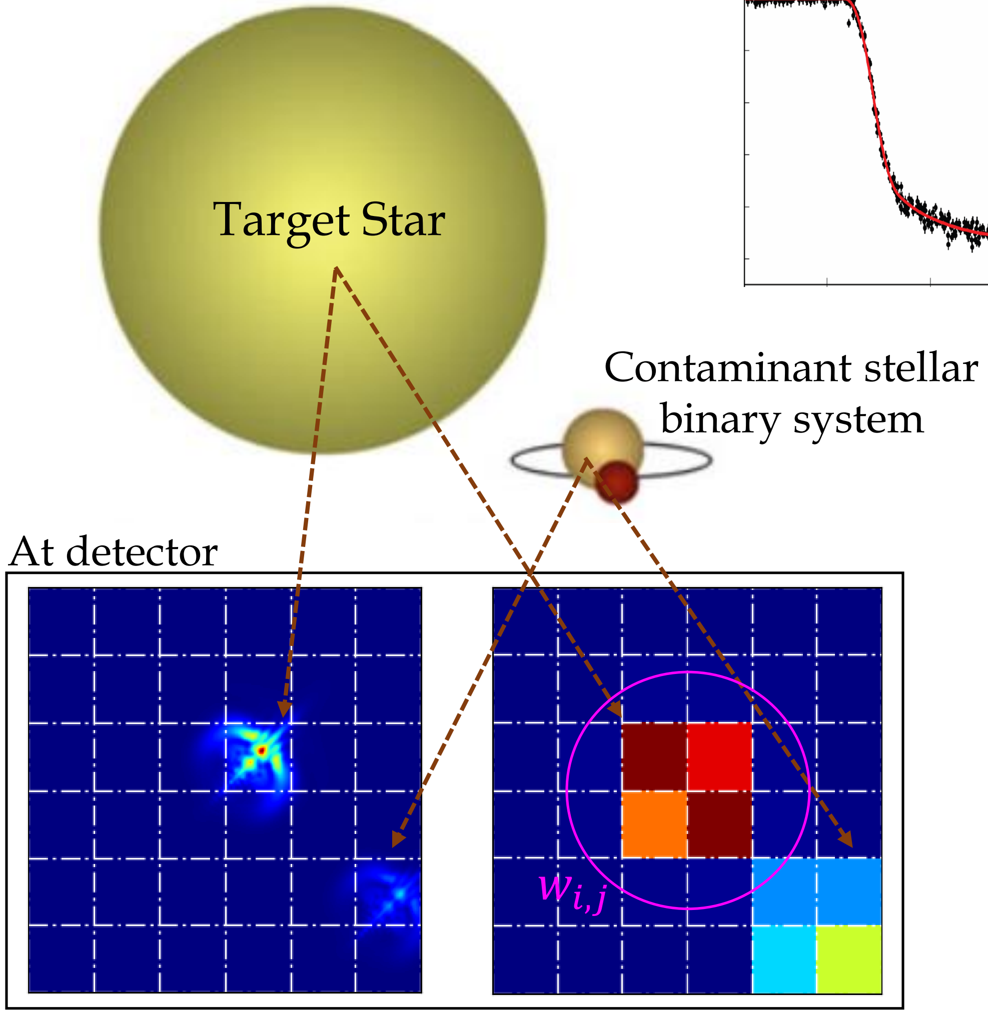

δ_{back} [mag]	Typical δ_{obs}		
	Gas giant	Neptunian	Earth
	0.01	0.001	80ppm
	Critical τ_C [%]	Critical τ_C [%]	Critical τ_C [%]
0.2	5.61	0.59	0.048
0.4	3.14	0.32	0.026
0.6	2.30	0.23	0.019
0.8	1.88	0.19	0.015
1.0	1.63	0.17	0.013

Conclusions from the presented analysis

- Contaminant rate is relevant on its own, NSR alone is not enough to guarantee adequate planetary science performance
- On-board photometry optimization shall not be performed only as function of the NSR (only parameter with formal specification)
- There is no silver bullet!
  No mask model can simultaneously minimize all performance parameters (NSR, flux variability, contamination rate, jitter etc.)

Strategies for choosing on-board masks to be studied

- 1. Hybrid masks
  - Advantage: reduces contaminant flux and flux discontinuities induced by jitter without sacrificing too much NSR
  - Drawback: sub-optimal performance for all parameters

Strategies for choosing on-board masks to be studied

- 1. Hybrid masks
  - Advantage: reduces contaminant flux and flux discontinuities induced by jitter without sacrificing too much NSR
  - Drawback: sub-optimal performance for all parameters

- 2. Multiple masks
  - Advantages: allows to extract the best from each mask model as a function of the contamination scenario
  - Gaia catalogue allows precise identification of contamination conditions, so the “best fit mask” could be determined on-ground prior to the observations
  - Drawback: consumes more on-board resources (to be quantified), need to check feasibility
  - Justifiability

Strategies for choosing on-board masks to be studied

- 1. Hybrid masks
  - Advantage: reduces contaminant flux and flux discontinuities induced by jitter without sacrificing too much NSR
  - Drawback: sub-optimal performance for all parameters

- 2. Multiple masks
  - Advantages: allows to extract the best from each mask model as a function of the contamination scenario
  - Gaia catalogue allows precise identification of contamination conditions, so the "best fit mask" could be determined on-ground prior to the observations
  - Drawback: consumes more on-board resources (to be quantified), need to check feasibility
  - Justifiability

- Obstacle:
  - No formal requirements for flux variability nor contamination rate

Next steps

- Study an alternative on-board mask strategy
  - Utilize GAIA catalogue to constrain contamination rate (e.g. first PLATO FoV)

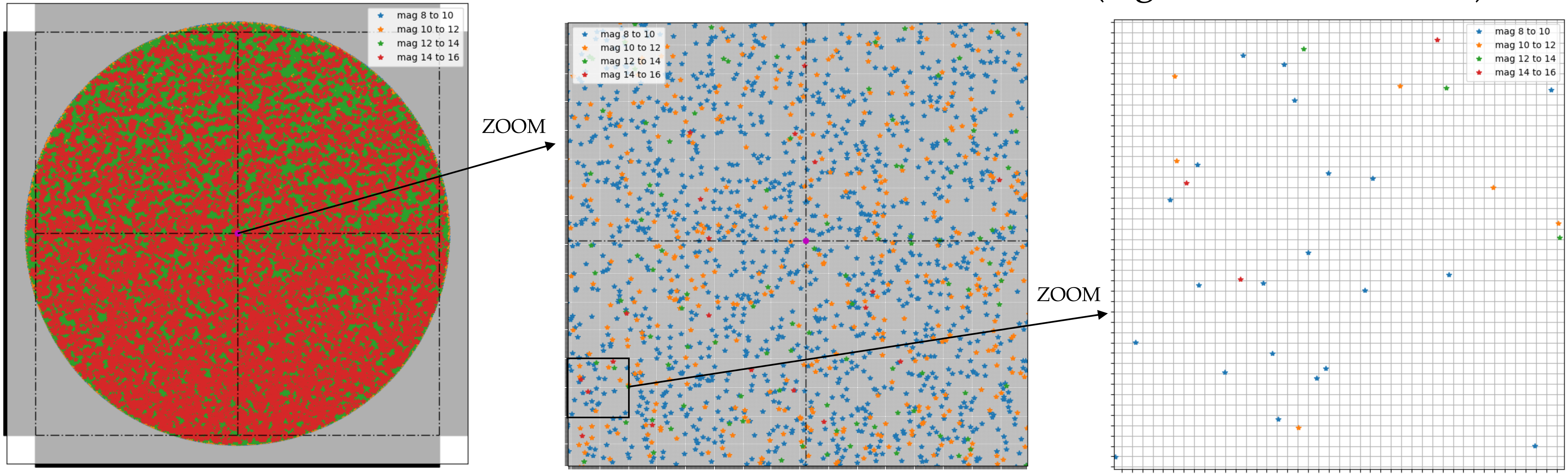

- Quantitatively constrain jitter sensibility and CCD effects in the masks performances analysis

TO BE CONTINUED…

The PLATO Mission: sky coverage

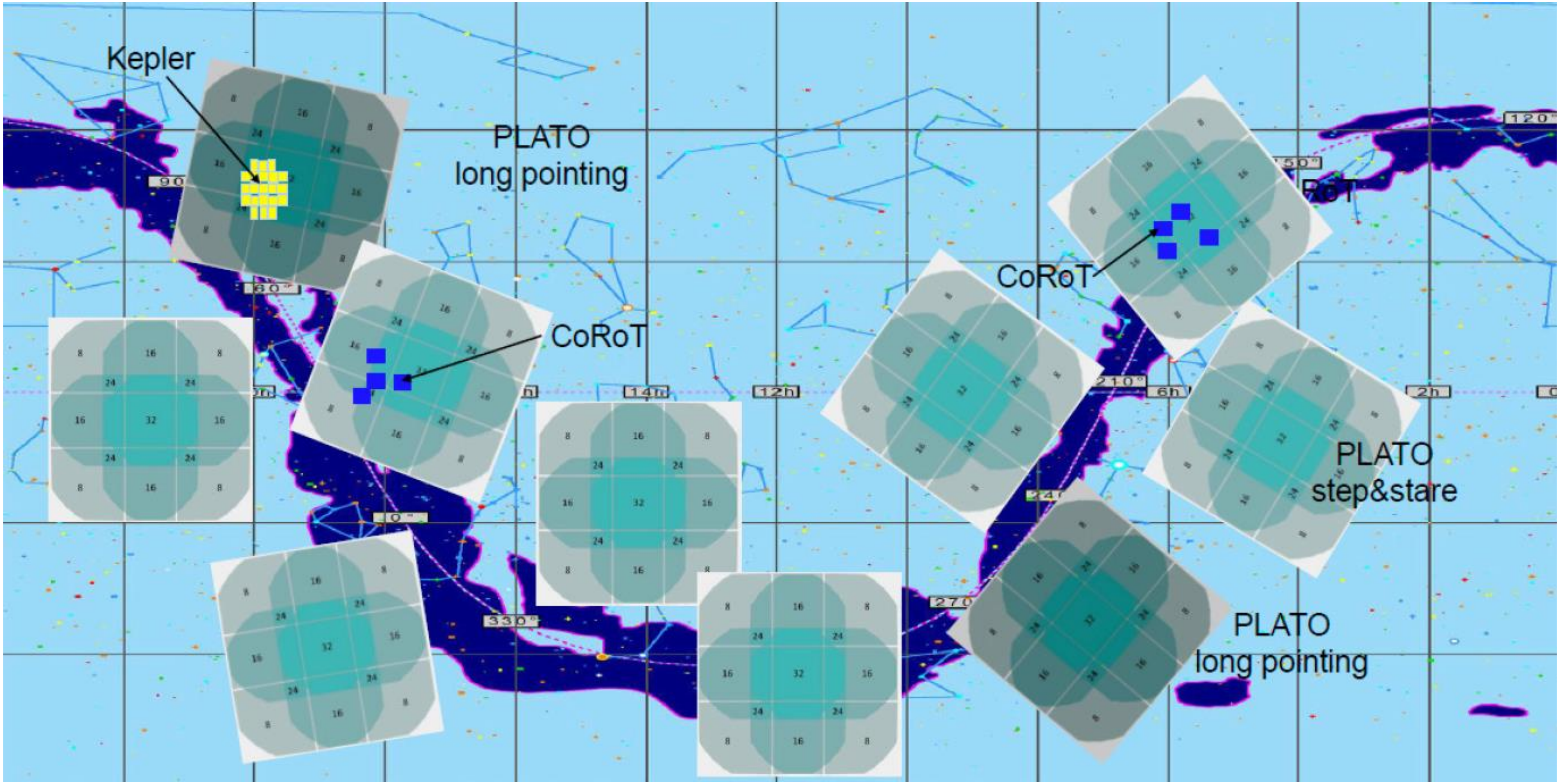

Analysis of masks performances: testing conditions and parameters

- Target star magnitude: 10.7 ; Target star temperature: 6000$[K]$

- Target star intrapixel positions:
  - Displacement range [-0.5, +0.5] w.r.t. pixel corner
  - Displacement step: 1/20 pixel

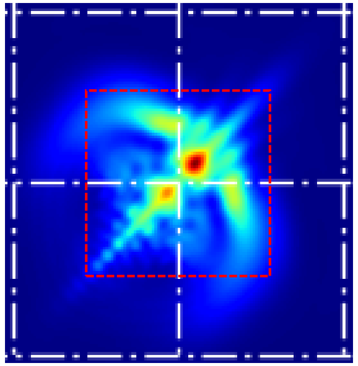

- Contaminant star magnitude: 11.7 ; Parasite star temperature: 6000$[K]$

- Contaminant star distance to target star: [0.5, 1.0, 1,5, 2.0, 2,5, 3.0] pixel(s)

Analysis of masks performances: testing conditions and parameters

- Photometric masks (5 models)
  - Optimal SNR binary
  - Optimal SNR weights
  - Optimal SNR symmetric Gaussian
  - Optimal SNR asymmetric Gaussian
  - Fixed-width symmetric Gaussian

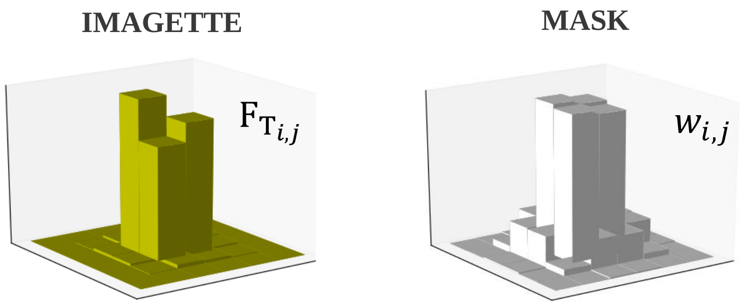

$F_{T_{i,j}}$ = target star flux at pixel (i, j)
$w_{i,j}$ = mask weigth at pixel (i, j)
$B_{i,j}$ = background noise at pixel (i, j)
$R_{i,j}$ = readout noise at pixel (i, j)

$$\mathrm{SNR} = \frac{\sum_{i,j}\left(F_{T_{i,j}} \times w_{i,j}\right)}{\sqrt{\sum_{i,j}\left(F_{T_{i,j}} \times w_{i,j}^2\right) + \sum_{i,j}\left(B_{i,j} \times w_{i,j}^2\right) + \sum_{i,j}\left(R_{i,j}^2 \times w_{i,j}^2\right)}}$$

- Exposure time: 21s ; background noise = 134[e^-/px/s]; readout noise = 60[e^-/px]
- No jitter ; no CCD effects (e.g. CTI, Brighter-Fatter, Diffusion)

Analysis of masks performances: results

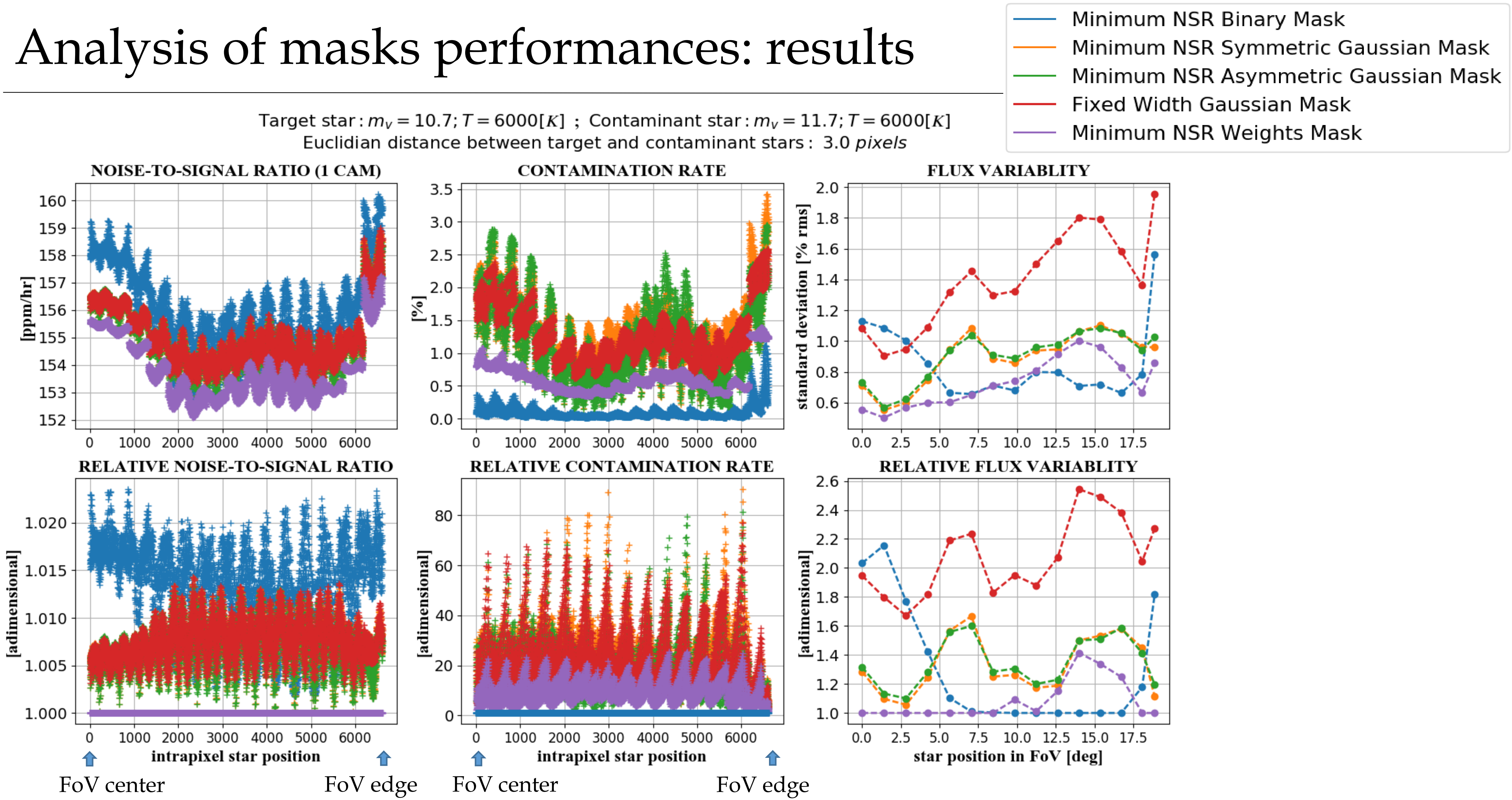

Analysis of masks performances: results

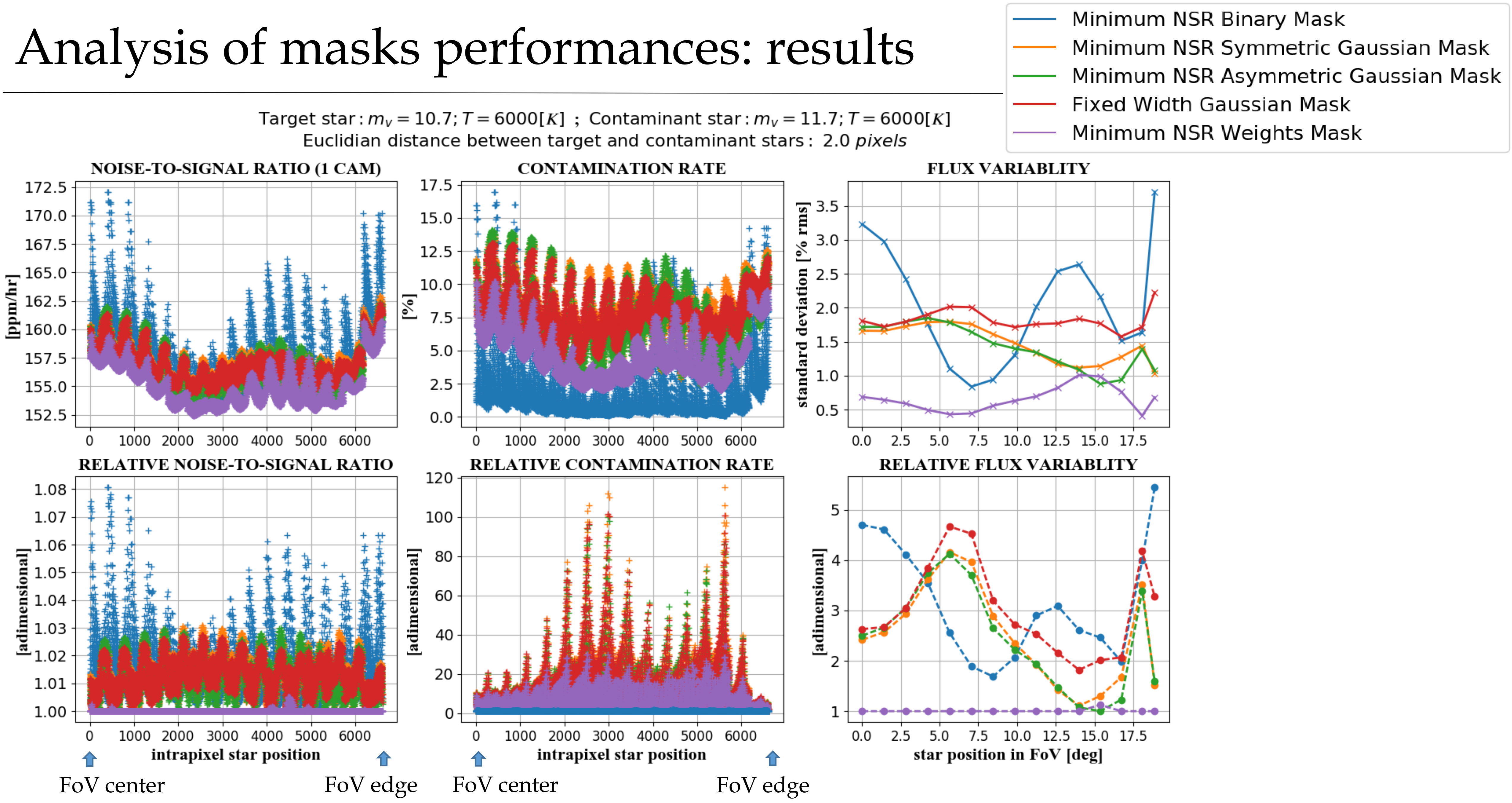

Analysis of masks performances: results

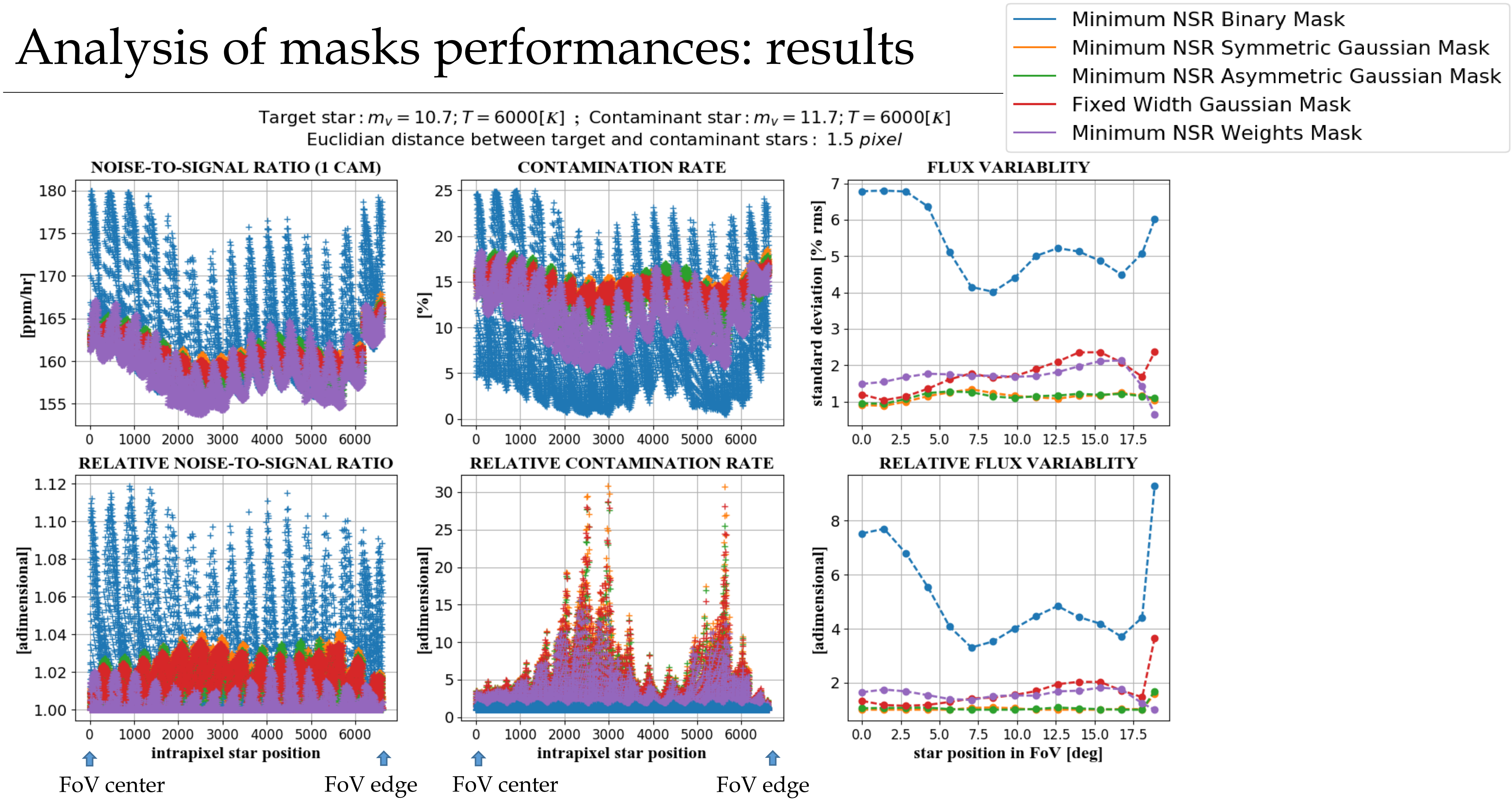

Analysis of masks performances: results

- Minimum NSR Binary Mask
- Minimum NSR Symmetric Gaussian Mask
- Minimum NSR Asymmetric Gaussian Mask
- Fixed Width Gaussian Mask
- Minimum NSR Weights Mask

Target star : $m_v = 10.7; T = 6000[K]$; Contaminant star : $m_v = 11.7; T = 6000[K]$
Euclidian distance between target and contaminant stars : 1.0 *pixel*

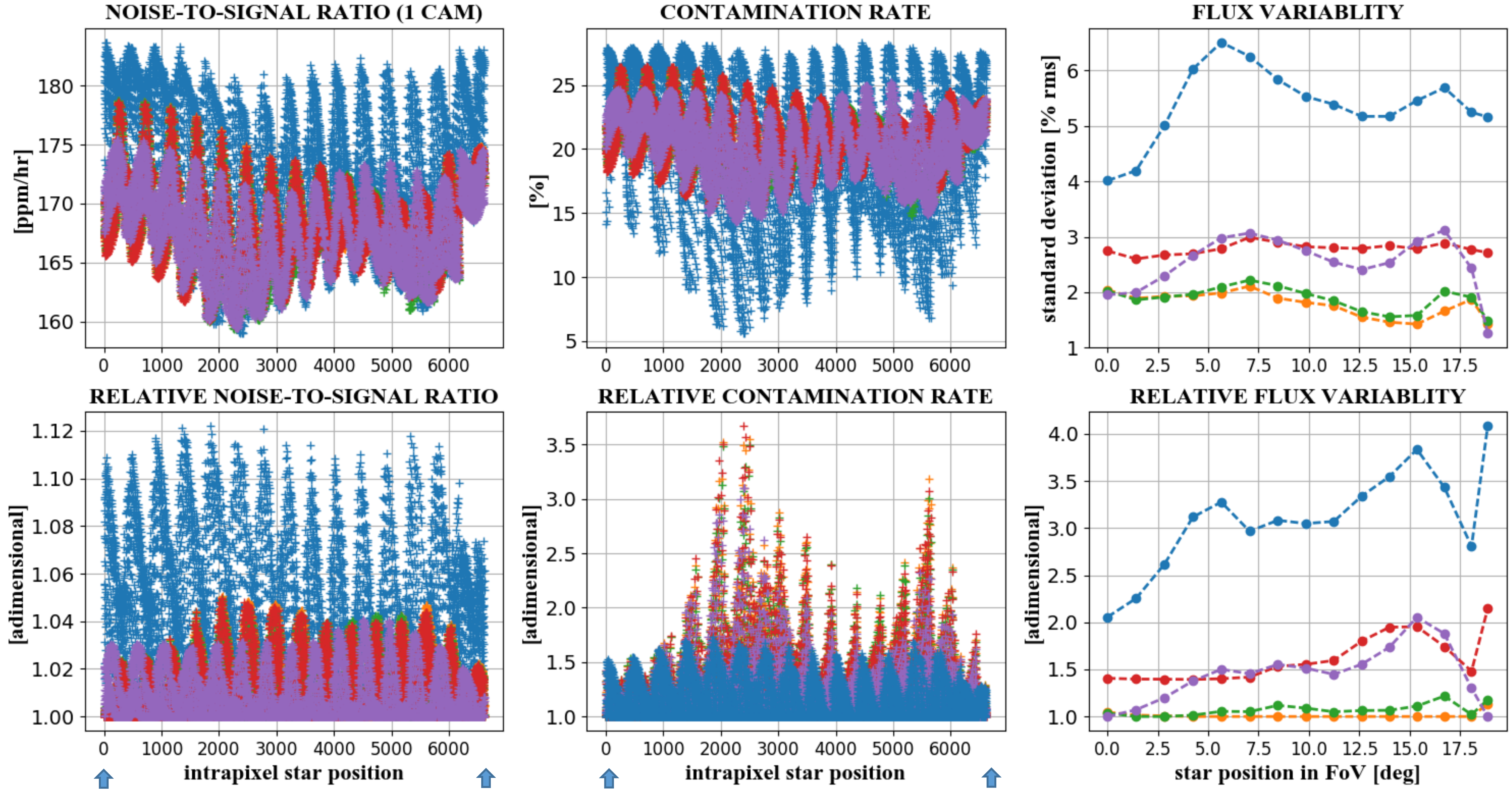

FoV center FoV edge FoV center FoV edge

Analysis of masks performances: results

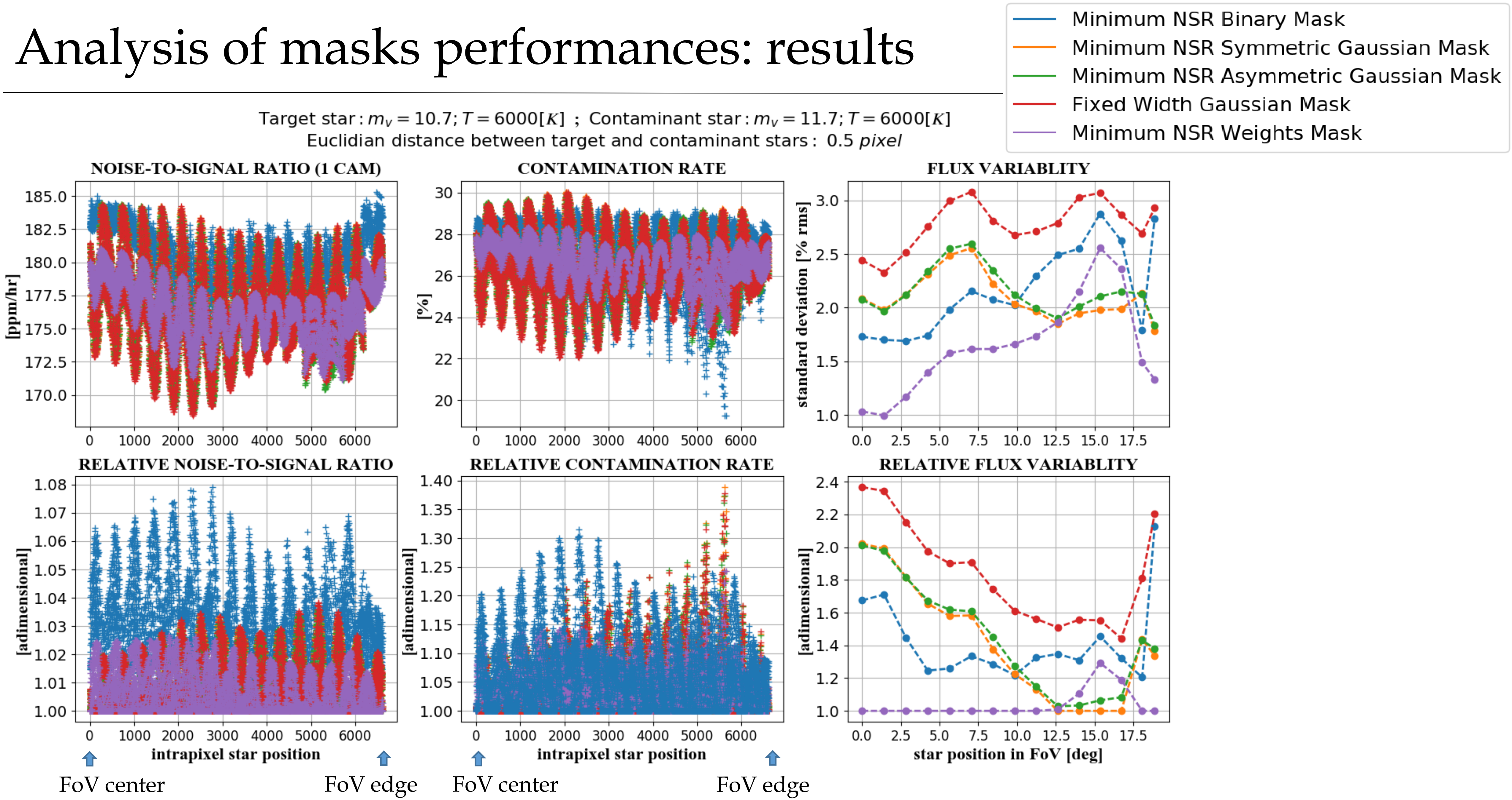

Conclusions from the presented analysis

Transit attenuation (or transit dilution)

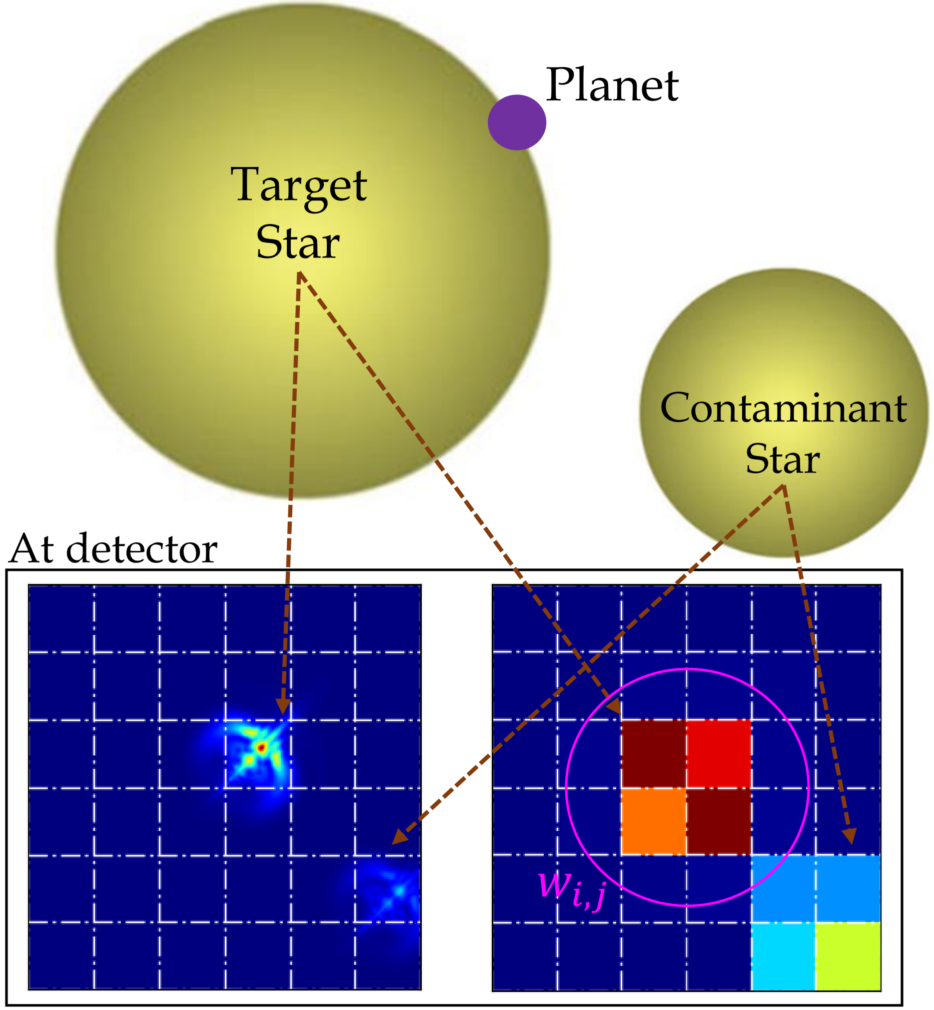

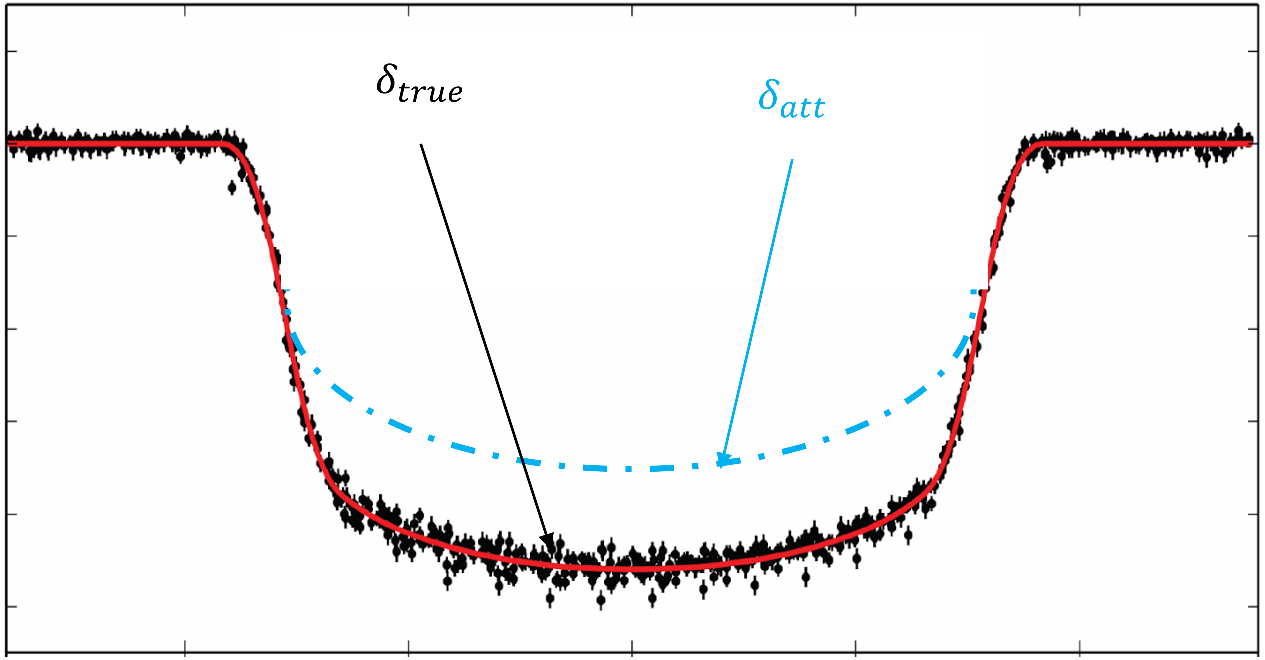

ATTENUATED TRANSIT DEPTH

$$\delta_{att} = (1 - \tau_C) \cdot \delta_{true}$$